Fall 1984

FLUORESCENT PROBE INVESTIGATIONS OF MICROENVIRONMENTS OF ANALYTICAL INTEREST (REVERSED-PHASE, POLYETHYLENIMINE, POLARIZATION)

SALLY DESMARAIS DOWLING
University of New Hampshire, Durham

Dowling, Sally Desmarais

FLUORESCENT PROBE INVESTIGATIONS OF MICROENVIRONMENTS OF ANALYTICAL INTEREST

University of New Hampshire PH.D. 1984

PLEASE NOTE:

In all cases this material has been filmed in the best possible way from the available copy. Problems encountered with this document have been identified here with a check mark _√_.

1. Glossy photographs or pages _____
2. Colored illustrations, paper or print _____
3. Photographs with dark background _____
4. Illustrations are poor copy _____
5. Pages with black marks, not original copy _____
6. Print shows through as there is text on both sides of page _____
7. Indistinct, broken or small print on several pages ✓
8. Print exceeds margin requirements _____
9. Tightly bound copy with print lost in spine _____
10. Computer printout pages with indistinct print _____
11. Page(s) _____ lacking when material received, and not available from school or author.
12. Page(s) _____ seem to be missing in numbering only as text follows.
13. Two pages numbered _____. Text follows.
14. Curling and wrinkled pages _____
15. Other _____

FLUORESCENT PROBE INVESTIGATIONS OF MICROENVIRONMENTS OF ANALYTICAL INTEREST

BY

Sally Desmarais Dowling
B.S., Northern Michigan University, 1976

DISSERTATION

Submitted to the University of New Hampshire
in Partial Fulfillment of
the Requirements for the Degree of

Doctor of Philosophy
in
Chemistry

September, 1984

This dissertation has been examined and approved.

W. Rudolf Seitz

Dissertation director, W. Rudolf Seitz, Professor of Chemistry

C L Grant

C. L. Grant, Professor of Chemistry

N. Dennis Chasteen

N. Dennis Chasteen, Professor of Chemistry

Gary R. Weisman

Gary R. Weisman, Associate Professor of Chemistry

Donald C. Sundberg

Donald C. Sundberg, Associate Professor of Chemical Engineering

July 3, 1984

Date

DEDICATION

This dissertation is dedicated to my motivating force for their irreplacable love: my husband, my sister, and my parents.

Bill withstood the agonies of being the "spouse of a graduate student" and always gave me the emotional support, patience, and practical perspective I needed.

Martha understood my moods, became my closest friend, and even acquired my household responsibilities to expedite my goal.

Mom and Dad demonstrated blind faith through the years in my ability to accomplish any goal I chose to pursue, and provided their unquestioning support for all my endeavors.

ACKNOWLEDGMENTS

For encouraging me to pursue a doctorate as I was about to write a master's thesis, I thank Drs. Tiny Grant and Rudi Seitz. As my adviser, Rudi was always ready with abundant ideas, animated explanations, and a level of excitement sufficient to overcome my initial hesitancy. The analytical faculty has guided my growth as a professional; and I credit Dr. Chris Bauer, Rudi, and Tiny for their continual encouragement, invaluable suggestions, and instruction.

Thanks to those fellow graduate students from whom I borrowed equipment, saught answers, and shared traumas. Special thanks are in order for the "analytical women": Carolyn Kheobian, Kathy Booth, and Irene McGee for moral support, sympathetic ears, and friendship.

The nonchemists who endured and valiantly tried to understand the process deserve particular mention. Shirley Provost provided constant friendship and her unparalleled skills in the preparation of this manuscript. Tish Davidson's sincere enthusiasm for my success was vital to my endurance. My husband's parents applauded each minor achievement and tolerated my demanding ambitions.

Without a research assistantship, I could not have achieved this goal in a timely fashion; therefore I am indebted to Rudi for obtaining a National Science Foundation grant and to the UNH dissertation fellowship fund. Moreover, I thank my husband, Bill Dowling, for providing a non-graduate student life style.

TABLE OF CONTENTS

LIST OF TABLES

LIST OF FIGURES

CHAPTER II

CHAPTER III

ABSTRACT

FLUORESCENT PROBE INVESTIGATIONS OF
MICROENVIRONMENTS OF ANALYTICAL INTEREST
by

SALLY D. DOWLING

University of New Hampshire, September, 1984

Fluorescent probes were applied to investigate three systems. Reverse phase chromatographic surfaces were studied using ion pairs. Variables were cation reagent structure and concentration, bonded phase (methyl, octyl, octadecyl, and phenyl), and solvent (water or methanol). Emission wavelength shifts for the anionic polarity probe, ANS, (8-anilino-napthalene-1-sulfonate) reflect the nature and extent of lipophilic interactions. Tetramethylammonium promoted ANS penetration into surface structure. Tetrabutylammonium overcame aqueous surface alkyl aggregation, which greatly enhanced ANS-surface interaction on C18. For the other phases at high cation concentrations there was lipophilic interaction between ANS and cation. High concentrations of small cations excluded ANS from the surface, as did all levels of trimethylmyristylamine cation. Methanol solvation reduced lipophilic interactions with alkyl surfaces. Pi-pi interactions were important with the phenyl surface. Results are consistent with the ion interaction retention model for ion pairing chromatography, which is based on double layer formation on a dynamic surface.

Polyelectrolyte-counterion binding strength and proximity were studied using a three component system: metals bound to polyethylenimine (PEI) and pyrenesulfonate counterion probes. Metals altered

rates of excited state processes and defined binding environment. Variables were net charge on metal and probe and metal-amine complex properties. Cu(II)-PEI efficiently and selectively quenched probes. Ground state dimerization in Zn(II)-PEI implied territorial binding involving lipophilic interactions with PEI and between probes was important. Quenching and excimer formation in Ag(I)-PEI were due to more than net charge since protonated sites did not alter emission.

Fluorescence polarization was used to detect intramolecular energy transfer between equivalent fluorophors in crown ethers, metal complexes, and simple organic molecules. Energy transfer randomizes the transition moment of emission relative to that of excitation, thereby decreasing polarization. In dilute glycerol solutions intermolecular depolarization is eliminated. A simple model based on Forster energy transfer theory was developed to distinguish molecules with different numbers of fluorophors and to obtain average angles between fluorophors, based on the extent of polarization differences.

CHAPTER I

INTRODUCTION

The phenomenon of molecular fluorescence is useful in a variety of contexts. Analytically, it has advantages over many other methods with respect to sensitivity, low detection limits, and selectivity. Fluorescence is also ideally suited to studying fundamental processes occurring during the fluorescent lifetime of excited molecules, 10-100 nsec (Hercules). Because the rates of excited state processes are often very sensitive to the medium around a fluorophor, fluorescence can be used as a probe of microenvironment. In view of these possibilities, applications of fluorescence are numerous and varied.

Fluorescence methods have been developed to measure trace levels of organic materials, inorganic and organic complexes, and inorganic ions (Parker). Although not all molecules of interest are inherently fluorescent, derivatization reactions are available to convert many kinds of compounds to fluorescent products (Seitz). This approach is widely applied in chromatographic detection. Fluorescence techniques are important tools in biomedical assays and biochemical research.

Fluorescent probes are also vital to enzyme, protein, and membrane studies. Fluorescent probes are introduced into a system to exploit the sensitivity of processes occurring between absorption and emission to microenvironment. The local environment influences fluorescent behavior by altering the relative rates of excited state

processes, as well as causing chemical interactions, electronic energy level shifts, and energy transfer.

The extent to which internal conversion is promoted is measured by the efficiency of quenching. Quenching usually involves interaction with a heavy atom or paramagnetic species present in the microenvironment. The decrease in fluorescence intensity observed depends on the concentration of quencher (in solution studies) or the extent of interaction between quencher and fluorophor (for probes bound within an environment containing a quencher).

Chemical interactions between probe molecules can be promoted by the microenvironment, providing the probe has a long fluorescent lifetime and proximity requirements are satisfied. When an excited and a ground state molecule combine, an excited state dimer (excimer) forms. Excimer emission peaks are characteristically broad and shifted to long wavelengths compared to the monomer emission peak. The relative intensities of monomer and excimer peaks depends on the proximity of bound probes. Extreme proximity is indicated if stable ground state dimers form. Dimers emit at the same wavelength as excimers, but the absorbing species are different; therefore they are identified by shifts in excitation spectra.

Emission wavelength shifts are also powerful indicators of microenvironment. Probes of this type are typically used as polarity indicators. The solvent or environment surrounding the fluorophor influences relative stability of ground and excited state electronic energy levels, manifested as wavelength shifts.

One process changing the relative orientation of electronic

transition moments during the fluorescent lifetime is energy transfer. This change in a probe can be measured using polarized excitation radiation; and resolving emission into parallel and perpendicular components in the fluorescence polarization technique.

This thesis consists of three sub-projects in which fluorescent probes were used to characterize microenvironments of interest in analytical chemistry. The three systems studied were: bonded phase chromatographic surfaces, polyelectrolyte-counterion binding, and intramolecular energy transfer.

Direct evidence regarding the nature of reversed phase hydrocarbon bonded surfaces under ion pairing conditions was obtained using a polarity probe. The need for a theoretical basis for retention mechanisms and a model for surface structure is evident from the conflicting reports in the literature. Variables of interest are the surface, the reagent ion structure and concentration, the solvent, and the solute structure. Surfaces studied were alkyl bonded phases of varying chain length (methyl, octyl, and octadecyl) and an aromatic bonded phase (phenyl). Commonly used quaternary ammonium ion pairing reagent cations were used to treat the surfaces with cation concentrations ranging from a fraction to an excess of bonded surface coverage. Water and methanol were used as solvents, since spectroscopic and chromatographic evidence points to a dynamic surface structure dependent on solvent polarity (Gilpin, 1982). The "solute" used was the fluorescent probe, 1-anilinonapthalene-8-sulfonic acid (ANS), which exhibits wavelength shifts as a function of polarity. These shifts are interpreted to indicate the nature and

extent of lipophilic interactions between the ANS and the reagent or surface studied.

The relative importance of lipophilic and electrostatic interactions involved in anionic probe binding was also considered in a polyelectrolyte-counterion binding study. A three component system was used, consisting of the polyelectrolyte polyethylenimine (PEI), a metal center bound to the polymer, and pyrene sulfonate counterions as probes. Electrostatic interactions between the metal-containing polymer and the anionic probe vary as a function of charge balance and coordinative saturation of the metal center, as predicted from the coordination number and complex stoichiometry of the metal with amine ligands. Cations used were copper(II), silver (I), zinc(II), and protons. Cu(II) and Ag(I) are both known to promote nonfluorescent decay from the excited state, while Zn(II) binds counterions in close proximity without quenching, promoting interactions between bound fluorophors and excimer emission. This method of altering the microenvironment of the probe counterion bound to the polyelectrolyte is an extremely versatile way to elucidate the nature of the binding site organization and interactions therein.

The third study involves intramolecular energy transfer depolaization between equivalent fluorophors on a given molecule. This process results in randomization of the transition moment of emission relative to the transition moment of excitation, which is detected by a decrease in polarization of fluorescence. It is possible to observe this process exclusively only if intermolecular processes are eliminated; therefore, dilute viscous solutions were used to elimiate

rotation and concentration depolarization. The systems studied were crown ether complexes, metal-fluorescent ligand complexes, and an organic bifluorophor. The information obtained demonstrates that intramolecular energy transfer can be used to distinguish binary mixtures without a separation and to obtain an average angle between transition moments of individual equivalent fluorophors on a single molecule.

CHAPTER II

SURFACE INTERACTIONS INVOLVING ION PAIR CHROMATOGRAPHIC PHASES

Introduction

The development of bonded phase columns has vastly expanded the capabilities of high performance liquid chromatography (HPLC). Reversed phase (RP) columns based on chemically bonding alkyl groups to silica through siloxane linkages are stable and provide a broad range of selectivity. The separation mechanisms and the physical nature of the bonded surfaces continue to be a subject of considerable interest and controversy. Various models of the alkyl surface, ranging from a rigid grass of isolated chains to a folded blanket of associated chains have been proposed (Gilpin, 1982).

Numerous spectroscopic and surface analysis methods have been employed in an effort to understand the microstructure of reverse phase chromatographic supports (Gilpin, 1983; Lochmuller; Bush). Only those techniques suitable for surface analysis in solutions of typical mobile phase composition provide information consistent with surface structure under chromatographic conditions. Furthermore, the technique must probe the solid-solution interface environment surrounding solutes and discriminate against bulk solution properties.

There has been substantial research to develop modifiers that alter the mobile phase or the surface so that alkyl-bonded phases may be applied to a wider range of solute types. Modifiers which enable RP columns to separate water soluble, ionic species are given the

general name "ion pair" reagents. These reagents are ionic molecules with hydrophobic tails, such as alkyl sulfonates or quaternary amines. They increase the retention of analytes carrying the opposite charge by promoting lipophilic interactions with the surface. Chromatographic results have served as the basis of models proposed for retention mechanisms in ion pair separations (Knox; Melander; Stranahan; Bidlingmeyer, 1979).

Our goal was to obtain direct evidence on the nature of surface interactions and how they vary with ion pair reagent concentration and the type of bonded surface using 8-anilino-napthalene-1-sulfonic acid (ANS) as our probe. It is nonfluorescent in water, while in other solvents its fluorescence wavelength is polarity dependent. ANS should be retained on alkyl bonded surfaces by an ion pair mechanism. Because it is a water soluble anion, a cationic ion pair reagent must be added to cause it to associate with the hydrophobic surface. Thus, ANS is uniquely suited to serve as a probe of microenvironment under ion pairing conditions.

The variables studied are those that are known to influence ion pairing separations. These include (1) the amount of cationic modifier because it affects the extent of electrostatic interactions, (2) the structure of the cation because it influences the retention behavior observed, (3) the nature of the bonded surface because each has unique lipophilic character and retention characteristics; and (4) the solvent because retention is a function of mobile phase solvent strength.

The modifier (reagent) concentration and size determine the

strength of electrostatic interactions and the nature of lipophilic interactions responsible for retention. Reagent chain length determines the relative importance of electrostatic versus lipophilic interactions (Stranahan). Bulky cations are known to dominate retention behavior, small cations provide higher capacity factors, and long chains inhibit solute mass transfer (Gloor). For that reason, tetrabutylammonium (TBA) tetramethylammonium (TMA), and myristyltrimethylammonium (MYR) were the quaternary amine cations chosen. Concentrations of these reagents ranged from below surface coverage of the bonded phase to a several molar excess.

The bonded phase itself also influences retention via lipophilic interactions with solution components. The nature of these interactions varies for each of the retention models that follow. The surfaces studied were methyl, octyl, octadecyl, and phenyl bonded phases. The surface structure is dynamic (Gilpin, 1982), with the orientation of the bonded group relative to the surface dependent on the alkyl chain length and the solvent.

The solvent effect was studied by comparing methanol versus water systems. Aggregated alkyl groups are thought to be oriented effectively parallel to the surface in water but become solvated in methanol and orient perpendicular to the surface (figure 1). This rearrangement affects the lipophilic character of the surface region.

Theory

Several models have been proposed to describe the mechanism of ion pair chromatography. The purpose of having a model is to understand the factors controlling retention and thus to guide the

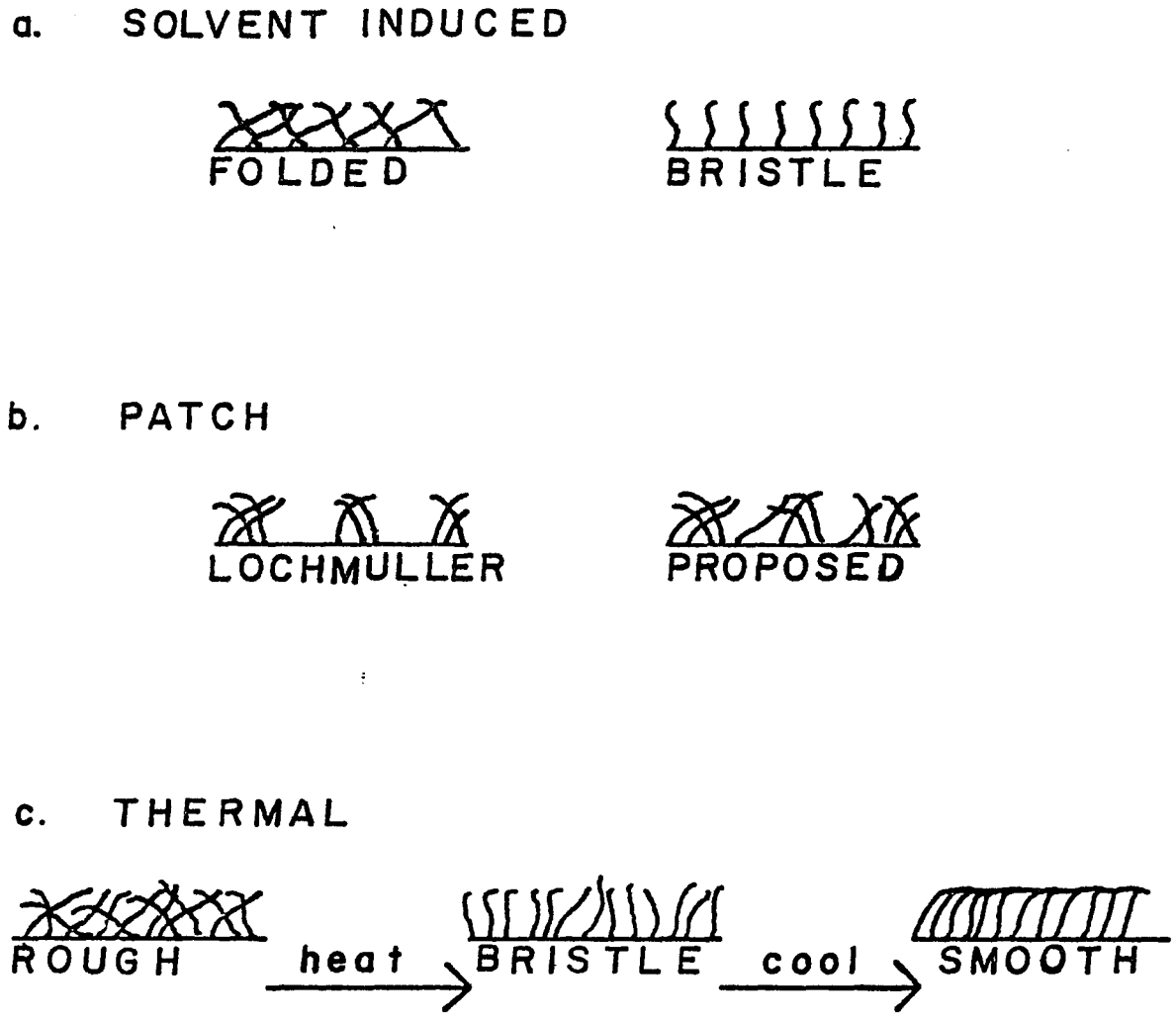

Figure 1. Dynamic reversed phase surface structure models.
a. solvent induced rearrangement b. patch model
c. temperature induced rearrangement

development of separation methods. The origin of ion pair techniques and terminology lies in ion pair liquid/liquid extraction. A water soluble ionic compound is extracted into an organic phase by using a counterion to form a neutral ion pair. The same counterions, or ion pair reagents, used in solvent extraction methods are applied to the chromatographic separation of ionic solutes. Accordingly, the first model proposed to explain the increased retention observed in ion pair chromatography was based on ion pair extraction theory.

Ion Pair Model

The ion pair model is represented in Figure 2a. It is based on the formation of an ion pair in the mobile phase. The ion pair travels through the column as a neutral molecule that is retained on the column by lipophilic interaction with the bonded alkyl phase. The nature of the lipophilic interaction with the stationary phase in this model involves both analyte and ion pair reagent molecules.

At best the simple ion pair model applies only to extremely limited cases. Conductivity experiments indicate that ion pairs do not form in typical mobile phases (Stranahan). Chromatographic experiments indicate that the stationary phase must be preconditioned with the ion pair reagent in order to achieve retention (Deming). The latter results imply that the reagent creates an ion exchange surface.

Dynamic Ion Exchange Model

This model, represented in Figure 2b, takes a completely different view of the mechanism of ion pair chromatography. The hydrophobic ion pair reagent is thought to adsorb onto the bonded phase,

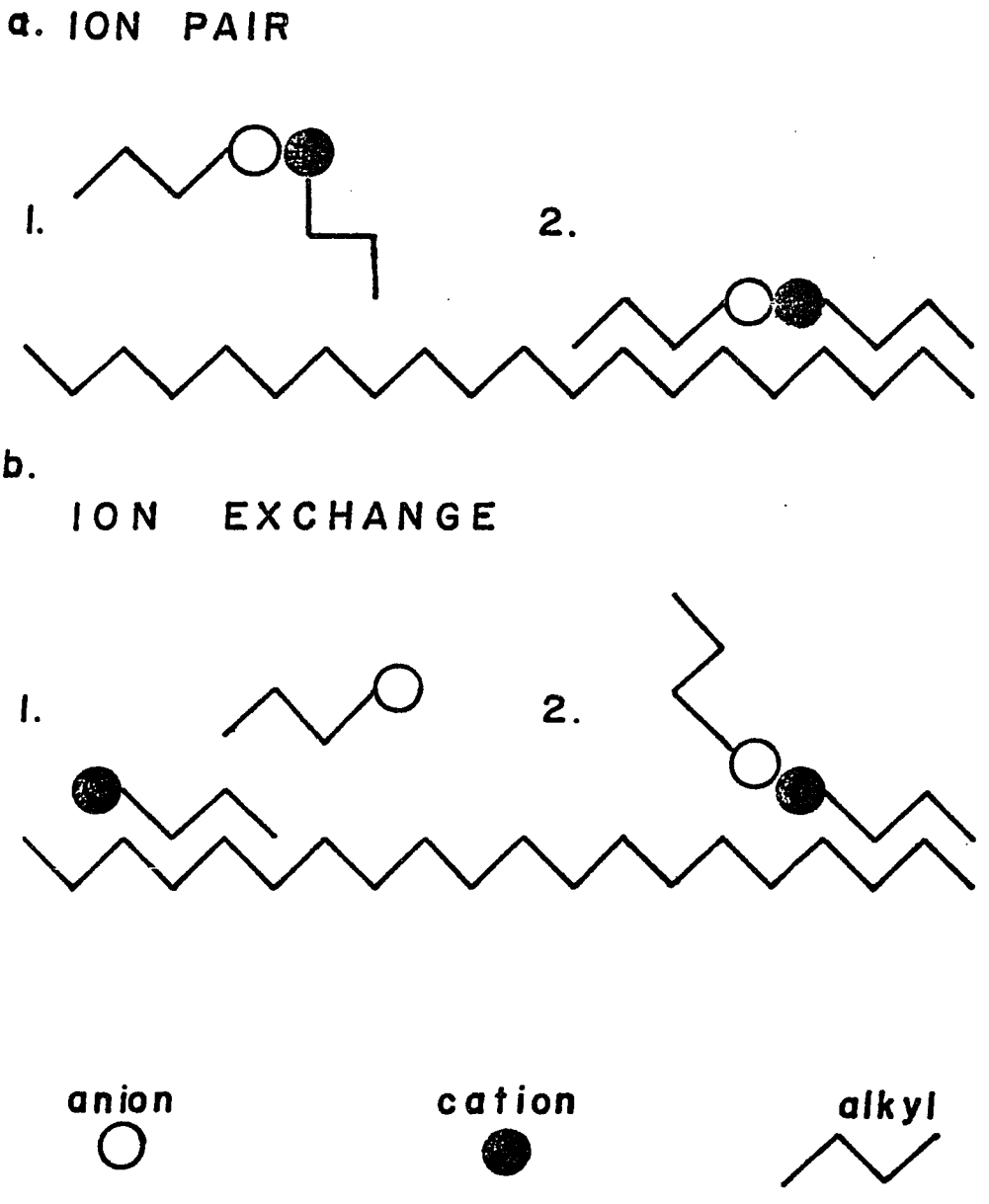

Figure 2. Simple retention models. a. Ion pair model 1) ion pair forms in solution and 2) partitions onto bonded phase b. Dynamic ion exchange model 1) reagent ion adsorbs, forming charged surface 2) solute ion is retained on charged surface by electrostatic forces

in effect forming a dynamic ion exchange surface (Knox). The primary retention mechanism for solutes of opposite charge is electrostatic attraction. The nature of lipophilic interactions in this model involves attraction of the hydrophobic portion of the reagent to the bonded phase. It does not allow for lipophilic interactions between the surface and the solute; and therefore does not explain selectivity differences between chemically different solutes of equivalent size and charge.

Ion Interaction Model

The ion pair and dynamic ion exchange models represent two extreme views. The shortcomings of the two simple mechanisms demonstrate the need to develop a more complex model that accounts for multiple forces that promote retention in ion pair systems. As a consequence, the ion interaction model, depicted in Figure 3, has been proposed (Bidlingmeyer, 1983).

As illustrated in Figure 3a, the reagent is attracted to the surface by lipophilic forces. The analyte is attracted to the adsorbed reagent by electrostatic forces. The neutral portion of the analyte is then close enough to interact with the surface by lipophilic forces. In this manner, a pair of ions, as distinct from an ion pair, interacts with the surface. The numerous factors contributing to distribution of species at the phase boundary are addressed in double layer theory.

Microelectrophoretic mobility data (Cantwell) were used to develop the double layer theory for ion pair retention. A primary layer is strongly held close to the surface by Langmuir-type

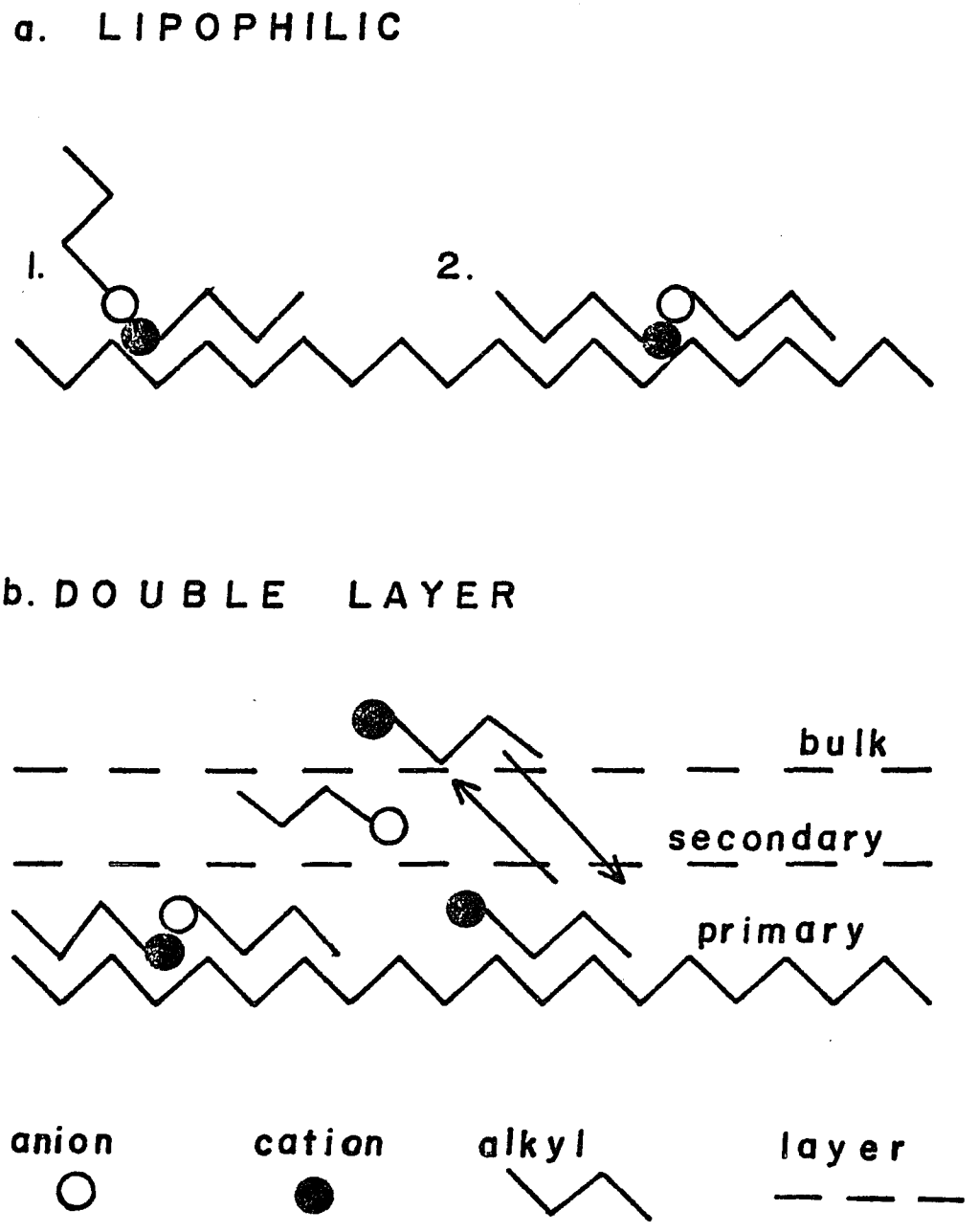

Figure 3. Ion interaction retention model. a. Lipophilic interactions 1) adsorbed solute-reagent ion pair forms 2) lipophilic attraction causes solute to interact with surface b. Double layer formation, based on competitive migration to primary solvent layer, after which surface interaction can occur

adsorption. The secondary layer has two regions: a compact layer and a diffuse layer of solvated counterions (Rosen). In Figure 3b, consider the distribution of a cationic ion pair reagent and an anionic solute. The adsorbed quaternary ammonium reagent ion is considered the primary part of the compact double layer on the hydrocarbonaceous surface. As cation concentration is increased, the diffuse secondary region of the double layer is compressed. This allows charge to build up on the surface. The solute and solvated inorganic counterions migrate from the bulk into the secondary layer.

The dynamic equilibrium within the double layer between the reagent ions and analyte ions comprises the electrostatic basis of retention in the ion interaction model. Other anions in the system compete with the analyte for residence in the diffuse secondary layer (Iskandarani). Selectivity is influenced by the relative size and concentrations of the solvated ion. High concentrations of reagent ions may exclude analyte from the primary layer, preventing lipophilic interactions.

However, even when reagent ion concentration nearly equals complete surface coverage, there is evidence of a significant interaction of solute with the surface which can best be explained in terms of solvophobic theory (Horvath). The driving force for this lipophilic association is a decrease in nonpolar surface area exposed to polar solvent. Surface tension is of paramount importance in this explanation. The charged surfactant (reagent) lowers surface tension by an amount that is proportional to the size of the ion (Tang). The extent of ionization, as determined by pH equilibria (Kong), must

also be considered. However, in the system studied, quaternary ammonium cations are aprotic and the sulfonated fluorophor is a strong acid. Thus, the chemistry will remain constant over a broad pH range (Jandera). Because reduction in surface tension by ion pair reagent is analogous to changing to a less polar solvent it is reasonable to expect that ion pair reagents cause the alkyl surface to reorganize.

Bonded Phase-Solvent Interactions

In a totally aqueous system the alkyl chains preferentially associate with themselves. In a relatively nonpolar organic solvent the chains are solvated and isolated from each other. Lipophilic interaction forces causing the solute to associate with the bonded phase vary with the nature of the surface morphology. The dynamic textural reorganization of the solvated surface (Scott; Wise) alters the extent of lipophilic interactions with solutes which can be detected by the fluorescence probe experiment.

The final state of the interfacial layers will be influenced by the size of the quaternary amine reagent molecule. Chromatographic data (Gloor) indicates that the structure of the quaternary reagent will influence retention. This implies that in the fluorescence experiment, the structure of the double layer and the surface on which it forms defines the environment of the probe.

Solutes that lie on the surface of a "blanket" or smooth phase will experience vastly different dispersive forces compared to solute molecules that vertically penetrate "bristles" of isolated bonded alkyls (Figure 1). Such differences should be apparent if the

solvent or cation changes the surface organization. The degree of penetration achieved is partly a function of chain length. A phenyl ring behaves as three methylene chain units (Tchalpa). In the case of aromatic solutes on an aromatic surface additional dispersion forces in the form of pi-pi interactions must be considered. If the diphenyl phase is smooth, ANS should adsorb in a configuration enabling maximum pi-pi interactions. Surface topology on the molecular level is not known, however.

The specific arrangement of the phase is dependent on the temperature history (Gilpin, 1981) of the surface as well as the bonded moiety and solvent. Surfaces heated in an aqueous environment rearrange from the collapsed or associated form to the bristle form with the introduction of sufficient thermal energy (41°C is the threshold temperature for C8). The structural change induced is described as depicted in Figure 1c (Hammers) as a transition from a rough associated layer to a bristle (at 79°C for C18) followed by collapse to a smooth associated layer upon cooling. Evidence for this model is demonstrated by entrapment of reversibly adsorbed solute molecules when heating is followed by rapid cooling. Thermally induced changes are reversible, but may retard equilibrium.

Surface Silanol Effects

Since ANS is a polarity probe, the activity of residual surface silanols as well as the lipophilic nature of the bonded phase must be addressed. This is especially important if the "patch" model of bonded phases is accepted (Figure 1b). In this model (Lochmuller) alkyl groups cluster to simulate liquid droplets and permit three

dimensional interaction with solute. The patch model is based on observation of excimer emission from pyrene chemically bound to silica. The inter-pyrene distance predicted for homogeneous distribution of bound pyrene is greater than the critical radius of interaction required for excimer emission. Thus, clustering is proposed at low bonded phase coverage.

The tendency of initial binding to be clustered is probably due to solubility considerations; on this basis the patches should expand to cover the surface completely as successive pyrene groups bind. The excimer emission is not surprising in view of the mobility of groups apparent in solid state 13C NMR experiments (Gilpin, 1983). There is no reason, therefore, to expect the termini of any bonded moieties of reasonable length to be separated by the average distance between points of attachment. A more reasonable interpretation (Figure 1b) is nonuniform distribution of bonded chain density with "holes" which are actually thin "patches".

Even free silanols left underivatized due to steric hindrance will not influence surface polarity in the solvents used. In water, transmission IR has been used to show that silanol sites are masked and inactive (Bush). Small amines bind to surface silanols and small ammonium cations may also act as silanol blocking agents (Bij). Residual silanols are also blocked by methanol, as demonstrated by 29Si and 13C cross polarization and magic angle spinning NMR (Bayer).

ANS Spectral Characteristics

The shift in ANS fluorescence as a function of polarity has been attributed to energy levels of the excited state molecule (Parker).

In water, pi*-n is the lowest transition, resulting in nonfluorescent decay due to the long lifetime of the excited state. Blue (short) wavelengths are indicative of low polarity, or predominately hydrocarbonaceous environment. For example, emission maxima are at 440 to 455 nm in aliphatic or aromatic solvents (Kosower). Shifts to longer wavelengths are indicative of increased polarity, or an environment dominated by a polar solvent. ANS emission in aliphatic alcohols is reported to range from 490 nm in methanol to 477 nm in n-butanol (Ware). Wavelength shifts observed for the systems presented here are interpreted in terms of environment polarity. Short wavelength emission maxima are taken to imply strong lipophilic interactions; in those cases the ANS is effectively isolated from interactions with the polar solvent.

Experimental

All chemicals were ACS reagent grade or better and used without further purification. The quaternary ammonium compounds used were: tetrabutylammoniumphosphate (TBA), 0.5M in water, pH 7.4 (Rainin, Woburn, MA); tetramethylammoniumhydroxide (TMA), 2.2M in methanol (Adlrich); trimethylmyristylammoniumbromide (MYR), powder, (Aldrich). 8-Anilinonapthalene-1-sulfonic acid (Aldrich) was prepared in water and methanol. Stock solutions were stored in the dark to prevent photodecomposition. Methanol was HPLC grade (Fisher). Water was doubly deionized and glass distilled.

Reverse phase supports were commercially prepared as monomeric materials. Methyl- (RP2), octyl- (RP8), and octadecyl- (RP18) silane phases were bonded to 10 μm LiChrosorb (BrownLee Labs, Santa Clara,

CA). The diphenyl (DP) phase was Supelco 5 μm LC-3DP. Carbon loading was determined on a Perkin Elmer Carbon-Hydrogen-Nitrogen (CH&N) analyzer (Table 1). The physical implications of the %C coverage by various bonded groups are represented in Figure 4. For the DP phase, since the surface area is quadruple that for the other phases, the relative coverage is even lower than shown.

Reverse phase materials (15 mg samples) were treated with cations in 200 μL methanol/water solutions in 1 dram vials. The resultant slurry was mixed thoroughly and gently dried in a vacuum oven at 30-45°C for up to 2 hours. Once dry, the preconditioned phase was packed into glass melting point capillary tubes. A small plug of silanized glass wool (Supelco) was used to contain the support in the tube. The capillary was then inserted in ANS solutions which were drawn into the tube by capillary action. This process was complete in 4-8 hours for methanol solutions and 16-72 hours for aqueous ANS solutions. Cation and ANS concentrations are indicated on the data tables.

Since ANS fluoresces weakly in methanol, care was taken to insure that the observed signal was only from surface-bound ANS. ANS concentrations were well below those needed to completely cover the surface. Direct visual examination indicated intense emission from particles and no visible emission from voids in the column. In systems showing wavelength shifts, there was no evidence of spectral broadening or development of shoulder peaks that would accompany a background due to non-surface bound ANS in methanol.

All spectra were obtained on a Perkin Elmer MPF-44E with slits

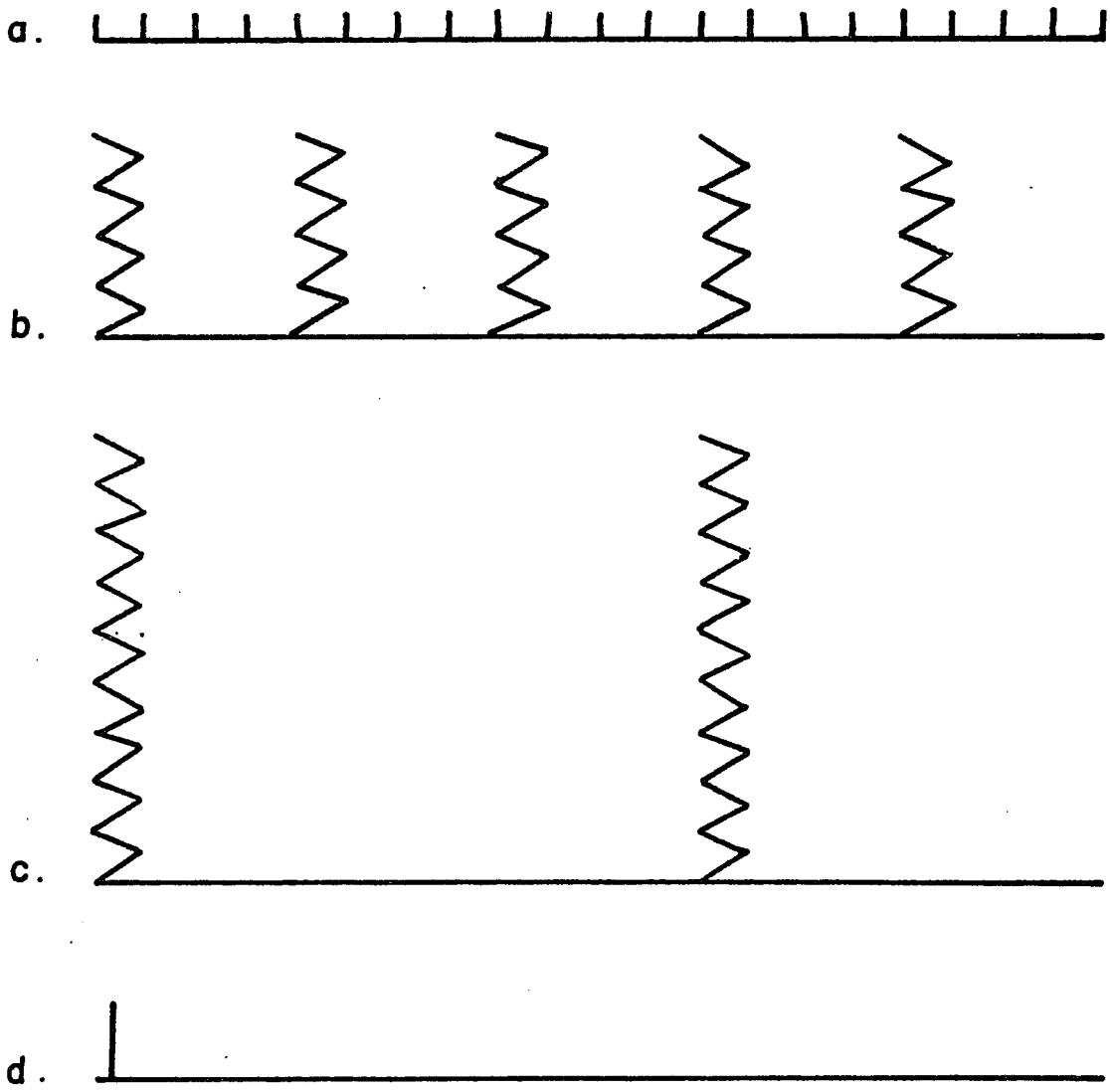

Figure 4. Relative coverage of bonded phase surfaces studied.
a. dimethyl (C2) b. octyl (C8) c. octadecyl (C18)
d. diphenyl (DP)

Table 1

Reversed Phase Surface Coverage

Phase	%C	µmole/mg
RP2	6.59	1.85
RP8	12.23	1.04
RP18	10.38	0.43
DP	3.80	0.10*

(*based on C:H ratio, DP phase is really trimethylphenyl-; this MW used to calculate molar coverage)

set at 2 nm using 378 nm excitation. Spectra are not corrected for variations in detection sensitivity with wavelength. Solution spectra were obtained at 10 μmole ANS and 1-1.3 mmole cation (maxima, Table 2) in a 1 cm quartz cell. Capillaries were reproducibly positioned in the beam by guiding them through a hole drilled in a fluorescence cell cover supported by the cell. Replicates of some surfaces were prepared and studied to determine the reproducibility of the preparation technique. The maximum variation associated with support preparation was ±3.5 nm.

Results

Wavelengths of maximum emission for all systems studied are presented in Tables 2-5. Pure solvent and blank surface data appear in Table 2. Wavelength shifts for various surfaces with TMA, TBA, and MYR are presented in Tables 3-5 respectively. Significant differences in wavelength are considered to be those deviating from the blank surface emission wavelengths by >7 nm. Significant shifts are underscored in data tables. Replicate data is presented in parenthesis, with individual determinations separated by commas.

Discussion

Blank Surface Wavelengths

Based on double layer theory, the blank surface wavelengths in Table 2b represent the bulky organic anion, ANS, adsorbed on the surface and surrounded by a diffuse secondary layer of solvated inorganic counterions. This is depicted in Figure 5. Since the concentration is very low, ANS is in an environnment dominated by solvent despite its proximity to the surface. Thus, the solvent

Table 2

Reference Emission Maxima

a. 10 µmole ANS + 1 mmole Cation in Solution

Cation	λmax (nm)	
	H_2O	MeOH
TMA	492	484
TBA	502	491
MYR	480	482
No Cation	---	475

b. ANS + Untreated Surfaces (Blank)

Surface	λmax (nm)	
	H_2O	MeOH
RP18	474	478
RP8	474	476
RP2	470	476
DP	474	474

a.

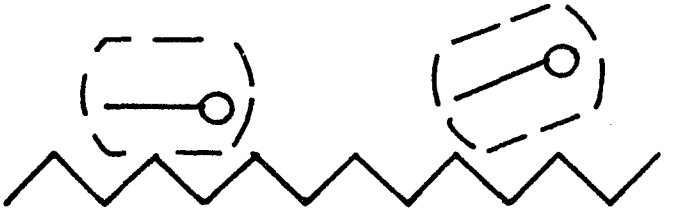

b.

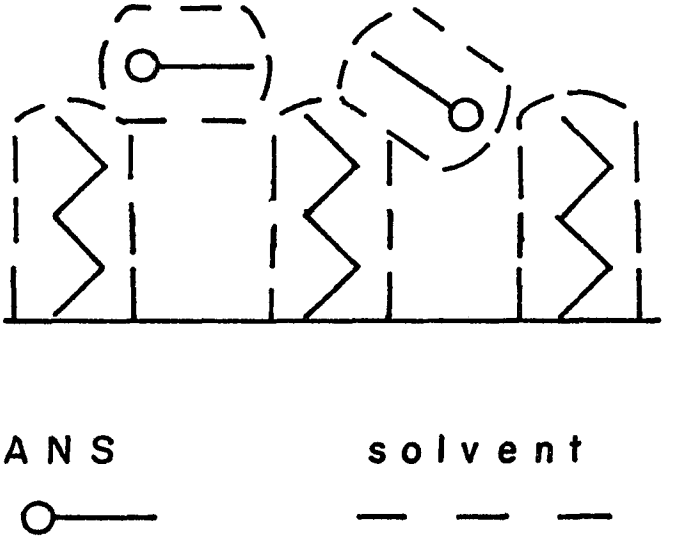

Figure 5. ANS interaction with blank surfaces.
a. in water, bonded surface is in folded orientation
b. in methanol, bonded surface chains are solvated

induced change from the "folded" to "bristle" orientation does not seem to have an effect in this context. The evidence for ANS-surface interaction is the blue shift relative to emission wavelengths for ANS ion pairs in solutions, shown in Table 2a. This shift is larger for aqueous conditions, implying that solvophobic forces in water cause ANS to interact more strongly with the surface.

The detectable emission from aqueous solutions of ANS and cations (Table 2a) indicates weak ion pair formation in water since free ANS would not fluoresce in water. However, this is observed only at millimolar cation concentrations, 100-fold greater than in surface experiments, and as such cannot be taken as evidence to predict solution phase ion pairing in the reverse phase system. In fact, only the myristyl cation demonstrates weak fluorescence with ANS in aqueous solution at the highest concentrations used in surface experiments. Thus, the limiting case of ion pairing in solution as the mechanism for ANS association with the surface is not important in this study. Instead, observed shifts are consistent with the ion interaction model.

Effect of Cation Concentration

In general, as the amount of ion pairing reagent increases, the wavelength of ANS emission shifts to higher values, indicating a more polar environment. Figure 6 depicts the high surface concentration cases. The wavelength shifts are consistent with concentration effects on the formation of the double layer. At high cation concentration the surface charge density is so high that it prohibits lipophilic interactions between the surface and ANS, thereby

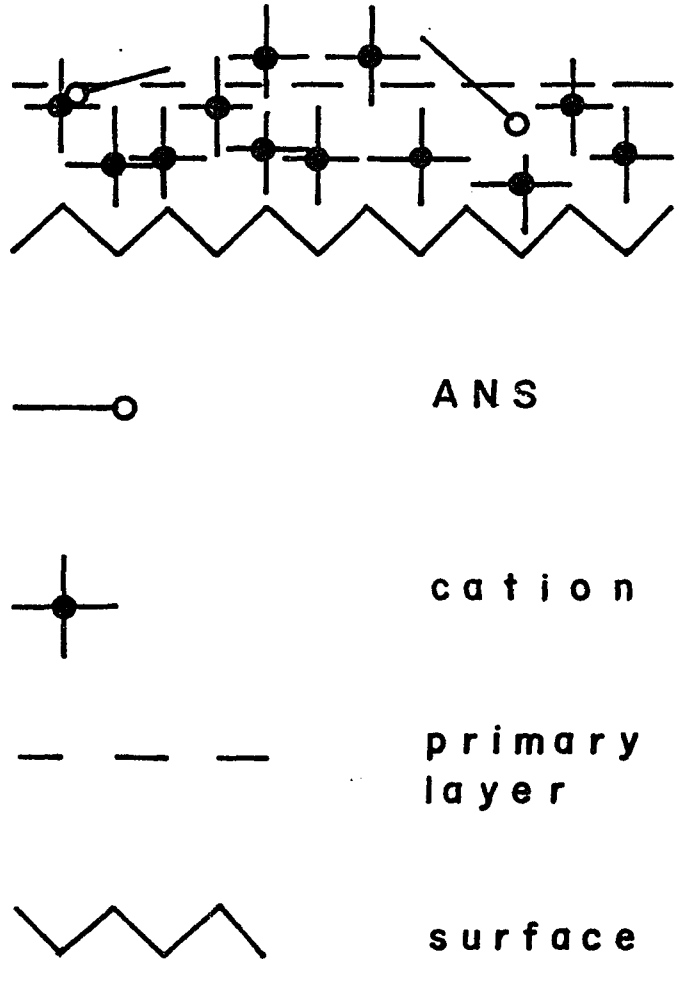

Figure 6. Effect of excess cation on ANS interaction with surfaces. Generalized bonded phase diagrammed represents all phases.

excluding ANS from the primary layer. TMA is particulary effective in preventing lipophilic interactions with the surface. In fact, at the highest TMA level in methanol the wavelength of maximum emission is the same as in pure methanol for all four phases, which indicates no lipophilic interactions whatsoever occur. In this case it may be valid to consider ion exchange theory as the limiting mechanism. The various systems at lower concentrations are discussed individually below.

Effect of Cation and Solvent

TMA in water. Tetramethylammonium results are presented in Table 3 and the implications of these results are schematically represented in Figure 7a. When cation concentration is below surface coverage, the double layer is diffuse and competing lipophilic forces become important. For 10 μmole TMA greater shifts for C18 and C8 compared to C2 indicate greater lipophilic interaction between ANS and the surface. The reduction in surface tension enables TMA to overcome self-aggregation of longer alkyl chains. This permits ANS to penetrate C8 and C18 surface structure (Figure 7a), as indicated by the greater shifts. When TMA concentration is less than the surface coverage on all alkyl phases, large shifts are observed for all phases (even C2) indicating strong lipophilic interactions. For the DP phase, the shift is also significant even though the DP surface coverage is low. In this system ANS is more likely to associate with DP than TMA because of pi-pi interaction forces; therefore it resides in the primary layer (Figure 7b).

TMA in methanol. Methanol solvates the C8 and C18 chains,

Table 3

Tetramethyl Ammonium Ion (TMA)
Treated Surfaces Emission Maxima

a. H_2O

Surface Bonded Phase	100 µmole TMA 100 nmole ANS	10 µmole TMA 100 nmole ANS	1 µmole TMA 2.5 nmole ANS
		λmax (nm)	
RP18	474	461 (459,463)	450
RP8	480	465 (462,467)	
RP2	472	468	446
DP	474	474	458

b. Methanol (MeOH)

Surface Bonded Phase			
		λmax (nm)	
RP18	484	476 (474,479)	469
RP8	486	474 (474,474)	468
RP2	483	470	467
DP	482	483	456

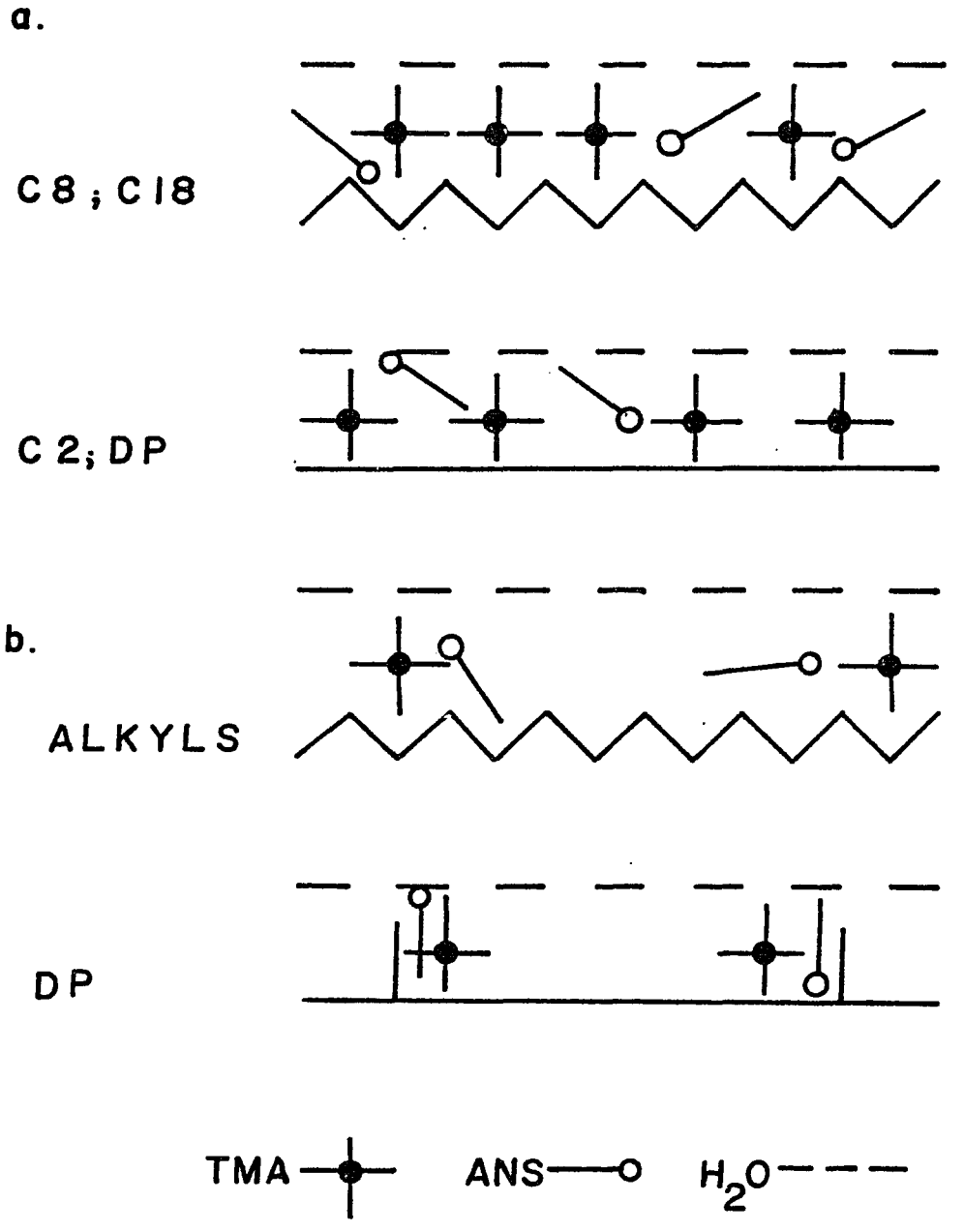

Figure 7. ANS in the presence of TMA in water.
a. 10 μmole of TMA b. 1 μmole of TMA

causing them to adopt the bristle rather than the folded configuration (Figure 1). The fact that wavelength shifts are smaller for TMA in methanol shows that the methanol tends to selectively solvate the alkyl-bonded phases. Solvation reduces the extent of lipophilic interactions between ANS and alkyl phases, although these interactions are still occurring. The exception is the diphenyl phase, where pi-pi interactions are possible. The wavelength shift is essentially the same for the DP phase in water and methanol, indicating that the ANS associates directly with the DP phase in both solvents.

TBA in water. Wavelength shifts for tetrabutylammonium are presented in Table 4 and the implications of these results are shown schematically in Figure 8. The most dramatic result is the large shift for the C18 phase at high TBA concentration. This shows that TBA has overcome the solvophobic forces causing C18 and C8 to aggregate in water, thereby drawing ANS into the phase and maximizing alkyl-ANS interactions. High levels of TBA also enhance lipophilic interactions on the other phases relative to TMA since ANS emission is at shorter wavelengths. However, the rearrangement observed for C18 is not possible for the phases with shorter bonded chains. At intermediate levels the shifts are less than at high TBA concentration. For the C18 phase, lower TBA is less effective at opening up the phase for penetration, although the shift is still large. For the other phases, this implies that the lipophilic interaction at high TBA is with TBA rather than the surface.

TBA in methanol. No significant shifts are observed for the

Table 4

Tetrabutyl Ammonium (TBA)
Treated Surfaces Emission Maxima

a. H_2O

Surface Bonded Phase	100 µmole TBA 100 nmole ANS λmax (nm)	10 µmole TBA 100 nmole ANS λmax (nm)	1 µmole TBA 2.5 nmole ANS λmax (nm)
RP18	444 (440,448)	454 (457,452)	450
RP8	470	467 (465,468,469)	457
RP2	466	474	462
DP	467	475	452

b. Methanol (MeOH)

Surface Bonded Phase	λmax (nm)		
RP18	477	474 (474,474)	468
RP8	478	474	472
RP2	482	475	469
DP	478	474	466

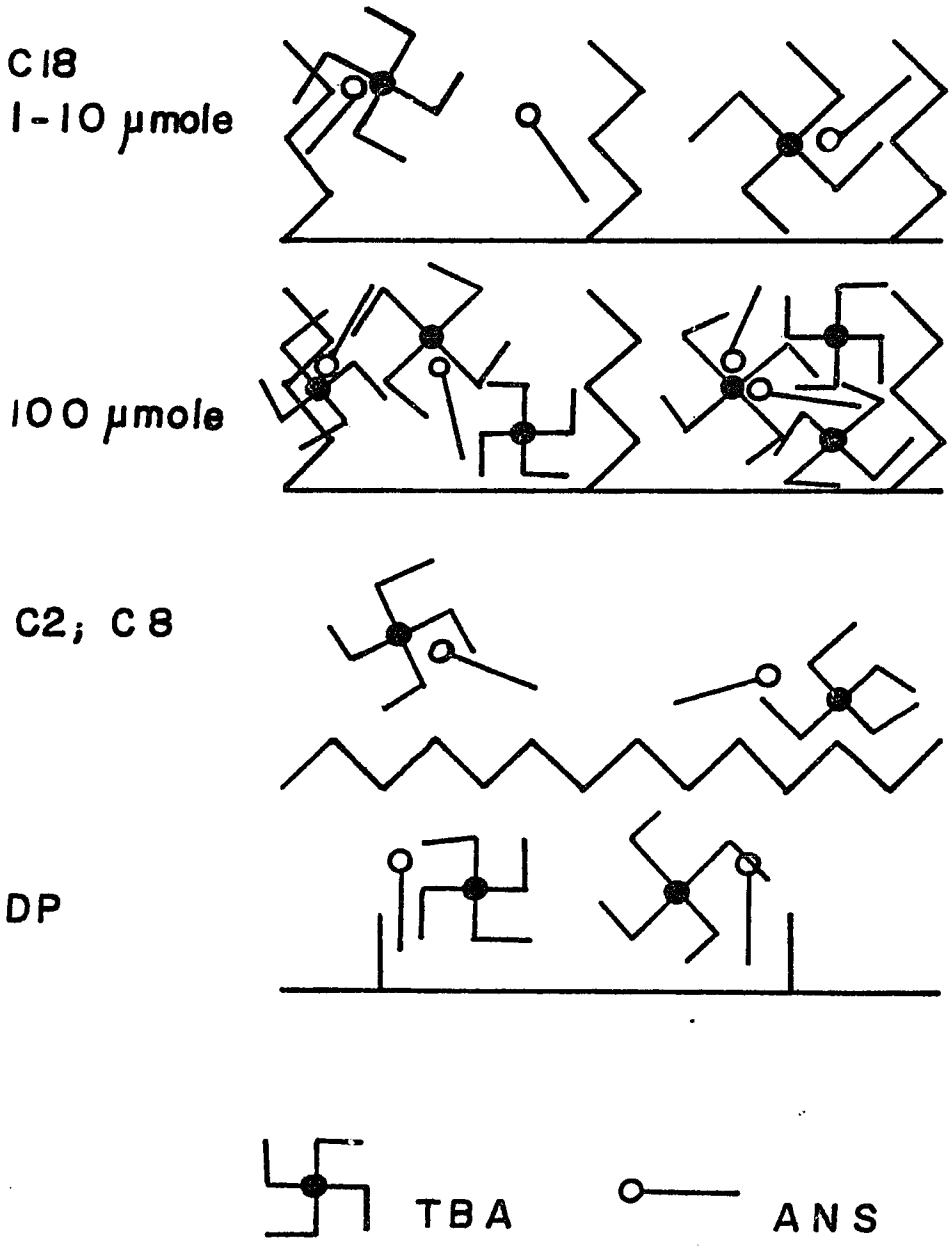

Figure 8. TBA in both water and methanol on specified surfaces.

ANS-TBA system in methanol. This emphasizes the importance of solvent when considering all competing processes in this system. The surface rearrangment occurs in pure methanol; and TBA does not promote any further change. ANS is in a predominately solvent environment, because strong solvent-surface interactions tend to exclude it from direct association with the hydrocarbon surface. The only important interaction is the pi-pi interaction with the DP phase, which is still quite weak.

Myristyl in water. Myristyltrimethylammonium results are presented in Table 5 and the implications are represented in Figure 9. The shape of MYR apparently prevents it from penetrating the aggregated alkyl chains, despite favorable alkyl interactions. The long chain apparently associates with the surface of the alkyl blanket, forming a surface layer. Electrostatic and lipophilic interactions are limited to the outer MYR surface coating and seem to be similar for all MYR levels.

Myristyl in methanol. In methanol, wavelength shifts are very small. Methanol preferentially solvates the surface and the myristyl alkyl chain, thus excluding ANS. The only exception to this is the DP phase where pi-pi interactions are important.

Conclusions

This investigation demonstrates the ability of surface active reagent ions to influence the structure of the bonded surface. The importance of the dynamic nature of the surface microstructure is emphasized by the ability of TBA to overcome the aggregation of alkyl chains and penetrate the surface. In addition to the nature of the

Table 5

Myristyltrimethylammonium (MYR)
Treated Surfaces Emission Maxima

a. H_2O

Surface Bonded Phase	100 µmole MYR 100 nmole ANS	10 µmole MYR 100 nmole ANS	1 µmole MYR 2.5 nmole ANS
		λmax (nm)	
RP18	469 (468,470)	466 (465,466,469)	467
RP8	468 (467,469)	467 (463,467,467)	
RP2	472 (468,475)	467 (465,468)	467
DP	475	475	467

b. Methanol (MeOH)

Surface Bonded Phase			
		λmax (nm)	
RP18	479	473 (472,474)	470
RP8	479	475 (473,476)	467
RP2	478	479	469
DP	478	472 (469,476)	458

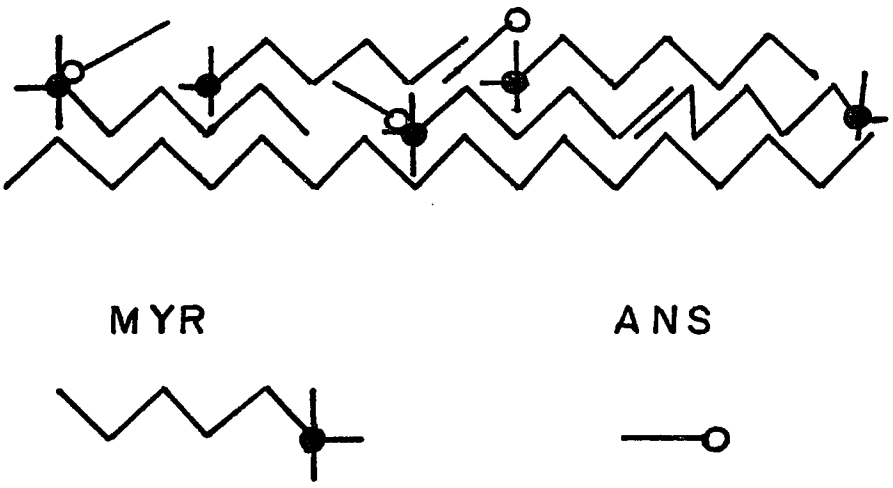

Figure 9. MYR under all conditions on generalized surface.

alkyl surface, mechanisms for retention in ion pair chromatography must take into consideration chemical interactions; and reagent concentration and structure. These factors all influence the nature of electrostatic and lipophilic interactions experienced by the solute in the interfacial double layer. The ion exchange limiting case of the ion interaction model is observed when large or highly concentrated cations shield the solute from experiencing the lipophilic surface attractions that draw it into the primary layer. The fluorescence probe results demonstrate why chromatographic observations are not all consistent with simple models for "ion pair" chromatography. Simple models require formation of either ion pairs in solution or a dynamic ion exchange surface. The ion interaction model is a more appropriate representation of the nature of lipophilic interactions responsible for retention, since the double layer theory on which it is based considers all competing processes involved and still allows for limiting cases.

CHAPTER III

POLYELECTROLYTE-COUNTERION BINDING

Introduction

Polyelectrolytes are known to bind organic reagents carrying the opposite charge (Manning). These associations are of interest to the analytical chemist for several reasons. Increasing the effective size of an organic reagent by binding to a polyelectrolyte allows the reagent to be immobilized by confinement behind a dialysis membrane. Changing the microenvironment of the reagent by association with a polyelectrolyte may modify the rates of excited state processes; thereby affecting luminescence behavior. In many respects, polyelectrolyte systems are similar to micellar systems which have been studied more extensively.

Polyelectrolytes have been demonstrated to surpass the ability of micelles (Turro, 1982, 2985) to enhance reactions (Ise) requiring specific orientation between counterions. This phenomenon has been attributed to the formation of micelle-like clusters within the polymer network (Sisido). Organic counterions associate with the charged sites on the polymer backbone by an ion pairing mechanism. In addition, there are lipophilic interactions between hydrophobic regions of the polymer and the organic ions. Both lipophilic and electrostatic forces are influenced by the polyelectrolyte backbone, the counterion structure, and the net charge associated with the

system components (Turro, 1983).

Luminescence probe studies have been used to characterize individual polyion-counterion interactions, as exemplified by the many studies of polystyrenesulfonate and polyvinylsulfonate. Concentration quenching (Taha) and excimer formation (Turro, 1982, 2985) have been observed and interpreted as evidence for formation of counterion clusters. Proximity of adjacent sites was further demonstrated by efficient quenching when emitter and quencher counterions of like charge bind to these polyions (Turro, 1982, 1535). Other anionic polyelectrolytes studied include polymethylmethacrylate, polyvinylbenzoate, (Martic) and polyperfluorosulfonates (Prieto). In all of these studies, the polymer-probe pair was selected specifically to promote the interaction of interest. Thus, synthetic preparations and additional experiments to separate variables associated with each component of the overall system were necessary. A counterion probe provides information about the type of binding interaction (lipophilic versus electrostatic), extent of and proximity due to clustering (territory formation versus specific site binding), and effect of charge type on the system.

Most of the polyelectrolytes studied have been anionic. The only cationic polyelectrolyte systems studied have been polyethylenimine (PEI) and functional derivatives thereof. However, reversal of charge does not change the nature of experimental results (Herkstroeter).

We have studied polyethylenimine-metal ion polyelectrolytes with pyrene sulfonate probes. This is a convenient and versatile system

because polyethylenimine (PEI) forms complexes readily with a variety of metals. The stoichiometry and strength of a given PEI-metal complex can be predicted from formation constants with model ligands.

The metal-polyelectrolyte has many attractive features for an investigation of the nature of the binding site organization and interactions therein. By varying the metal it is possible to influence the rates of excited state processes. Specifically, Cu(II) quenches fluorescence by enchancing the rate of internal conversion; and Ag(I) promotes intersystem crossing which induces phosphorescence in rigid systems. In addition, the charge on the metal center can be varied by using different metal ions; and the accessibility of the charge to counterions can be varied by choosing metals with different coordination numbers.

Pyrene sulfonates were chosen as fluorescence probes because they are sensitive to quenching and can provide proximity information via the extent of excimer formation. Using a fluorescent probe as the bound counterion provides direct information about the nature of the binding microenvironment. Mono- (PySA) and tetra- (PySA4) pyrene sulfonates were both employed as probes to determine the influence of counterion charge on binding.

Polyethylenimine

Polyethylenimine (PEI) is a water soluble branched chain polymer composed of $-(CH_2CH_2NH)-$ monomer units. Protonation of the amines makes PEI a weak polyelectrolyte in its native form. The functional groups of the polymer consist of approximately 25% primary, 50% secondary, and 25% tertiary amine groups (Davis). PEI is a weak base

although only 70% of the nitrogen groups are available for acid/base reactions due to the tertiary nitrogen branching (Encyclopedia of Polymer Science). However, because interactions with the native PEI backbone are hard to predict and control, the backbone is often modified synthetically to produce polymers with very specific binding interactions (Klotz). For example, at very low loading of covalently bonded pyrene on the PEI backbone (0.1%), the appearance of excimer emission was attributed to clustering (Pranis). A better way to modify the system is by forming complexes of metal ions with the amines acting as nitrogen ligands. Branching results in stronger binding (Vink). Anionic fluorophors bind to cationic metal centers on the polymer to form an infinite number of three component systems.

Pyrene

Pyrene is widely used as a fluorescent probe of microenvironment (Gordon). Since pyrene has a long fluorescence lifetime, it is sensitive to quenching. In addition, it is possible to observe excimer fluorescence when probes are in close proximity. An excimer results from the interaction of an excited state molecule of pyrene with a ground state molecule to form an excited state dimer, which then emits at a longer wavelength than the monomer. Excimer intensity has been analyzed to evaluate the extent of interaction between fluorophors covalently bonded to polyelectrolytes (Herkstroeter).

True excimer emission is observed if sites are reasonably close together but not close enough to form stable ground state dimers, whereas ground state dimerization requires extreme proximity. Ground state dimer and excimer have identical fluorescence emission but can

be distinguished by differences in excitation spectra. Ground state interactions, which do not normally occur in solution, have been reported between pyrene groups in polyelectrolyte structures (Herkstroeter).

Binding to polyelectrolyte has also been demonstrated to reduce the translational mobility of counterions (Zero). If the polyelectrolyte environment is sufficiently rigid it should be possible to observe phosphorescence at even longer wavelengths than excimer emission. Since phosphorescence lifetimes are extremely long compared to fluorescence, competing nonradiative processes usually prohibit observation of solution room temperature phosphorescence.

Experimental

All chemicals were reagent grade and used without further purification. Sulfonated pyrenes were obtained from Molecular Probes, Inc. The structure of pyrene and the position of sulfonate substituents on both fluorophors are shown in figure 1. Inorganic salts, TRIS (tris(hydroxymethyl)aminomethane, THAM) buffer and standard metal solutions were obtained from Fisher. Water was doubly deionized and glass distilled.

Tetraethylenepentamine and polyethylenimine were obtained from Adrich. Polyethylenimine, nominal MW 40,000, was received as 50% aqueous solution. The actual concentration, determined by elemental analysis, was 49.3%.

Potentiometric titrations were performed to determine the stoichiometry and strength of metal binding to PEI. Standard metal solutions and PEI were buffered with TRIS to provide constant

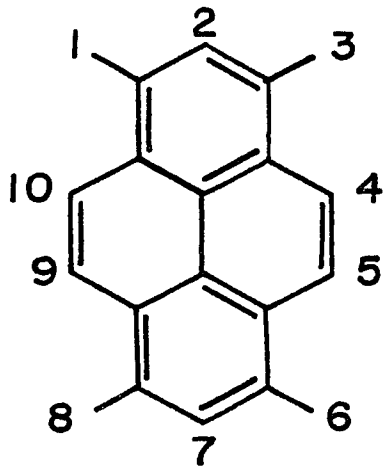

PySA

1- SO_3^-

PySA4

(1, 3, 6, 8) - SO_3^-

Figure 1. Structures of pyrene sulfonate probes.

pH 7.42 in 0.1M $NaNO_3$ which was used to maintain constant ionic strength. A combination glass electrode was used to monitor pH. Free Cu(II) ion activity was measured with a solid crystalline (CuS) Orion electrode, sleeve type Orion standard calomel reference, and an Orion Digital Ionanalyzer/501 meter. A piece of silver wire versus the SCE reference with a Keithley digital multimeter was used to measure free Ag(I).

Fluorescence titration curves were obtained with a Perkin Elmer MPF44E in 1 cm quartz cells at a constant PEI concentration corresponding to 0.1mM monomer units and at constant fluorophor concentration (0.01mM) to keep the inner filter effect constant. All experiments were conducted at pyrene concentrations below 1.0mM to prevent excimer formation in solution, independent of interactions with the polymer. Metal standards in TRIS buffered 0.1M $NaNO_3$ and 0.1M $NaNO_3$/TRIS blank solutions were added in appropriate volumes to prepare constant ionic strength solutions with varying metal to nitrogen ratios.

Results and Discussion

Potentiometry

The curve for PEI titrated with Cu, Figure 2, indicates that the binding of this ion to the polymer is strong. The equivalence point, located from a second derivative plot, corresponds to 5.6 monomer units per Cu(II). If Cu(II) is bonded to four N units, which is a reasonable coordination number based on the well known $Cu(en)_2$ complex, then it implies that there is a chain containing an average of 1.6 monomer units between adjacent Cu(II) sites. The formation

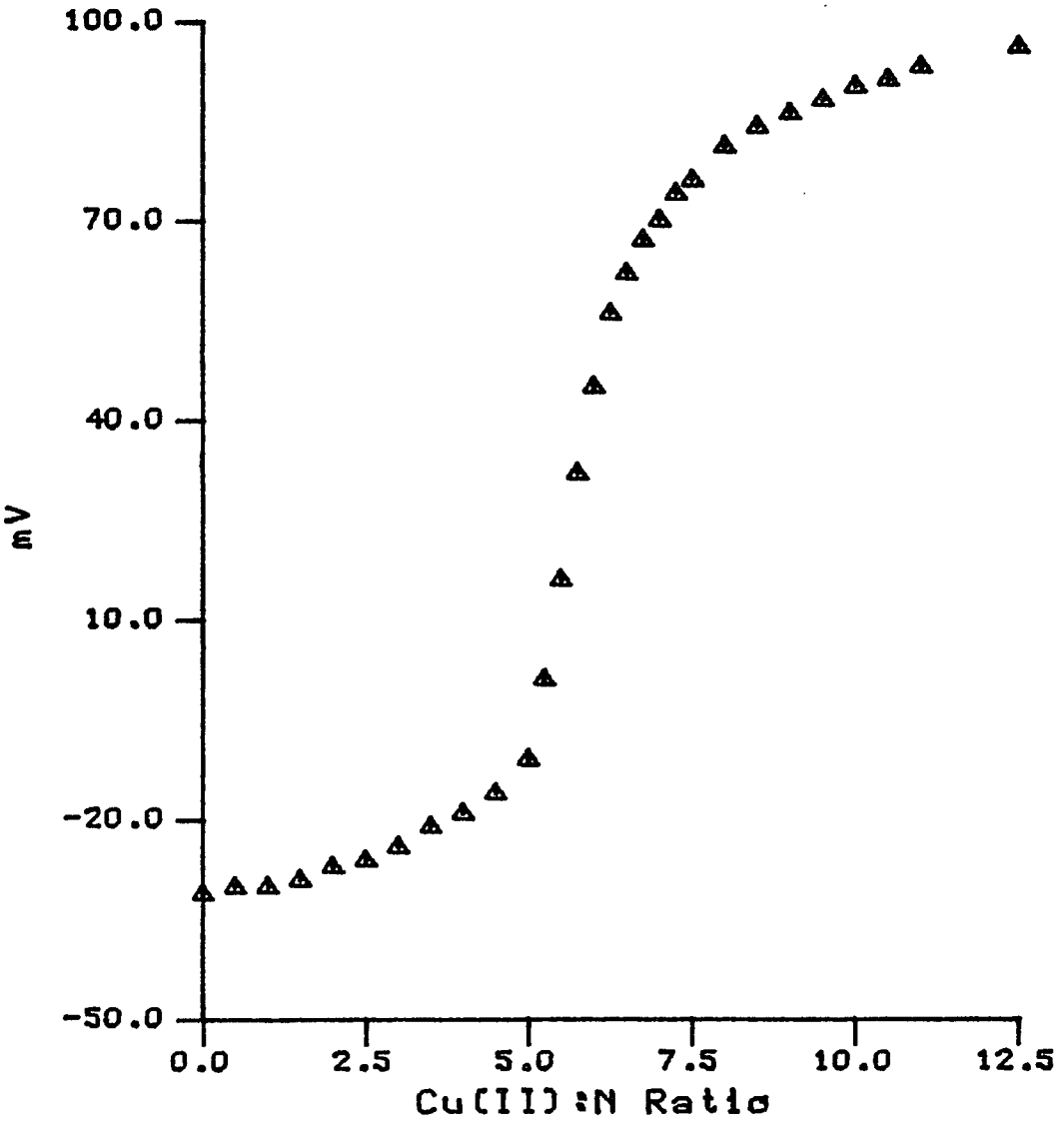

Figure 2. Potentiometric titration of PEI with 1 mM Cu(II).

constant estimated from this data, log Kf=13, is much lower than the literature value (Smith) for (Cu)en_2, log Kf=20.

The titration data for Ag(I) is presented in Figure 3. The shape of the curve indicates a nonhomogenous distribution of binding sites. The absence of a large break in the curve indicates that Ag(I) is bound much more weakly than Cu(II). The equivalence point, from the second derivative plot, corresponds to an average of 4.3 monomer units per Ag(I). In view of Ag(I) coordination chemistry it is likely that Ag(I) is bound to an average of two N units.

The pH titration curve, Figure 4, indicates that the polymer is completely saturated with protons at pH 2.5. The equivalence point corresponds to 1.6 monomer units per H, which is consistent with the 70% protonation expected for PEI. The native polymer is partially protonated in the pH 7.42 TRIS used for fluorescence titrations.

Titration information was not obtained for Zn-PEI. There is no potentiometric method for Zn(II) and discrimination between free and bound Zn(II) by polarography was also ineffective since the polymer adsorbed on the surface of the dropping mercury electrode, resulting in irreversible waves. The trend for the other metals with PEI corresponds to binding strength and stoichiometry with the simple ligand ethylenediamine (en). Therefore, literature data for en was used as the basis for assumptions about the binding of Zn to PEI. Zn(II) binds three en ligands, whereas Cu(II) binds only two. In addition, the overall formation constant for $Zn(en)_3$ is much smaller than Kf for $Cu(en)_2$. Overall Log Kf values are 14 and 20, respectively for these en complexes (Smith).

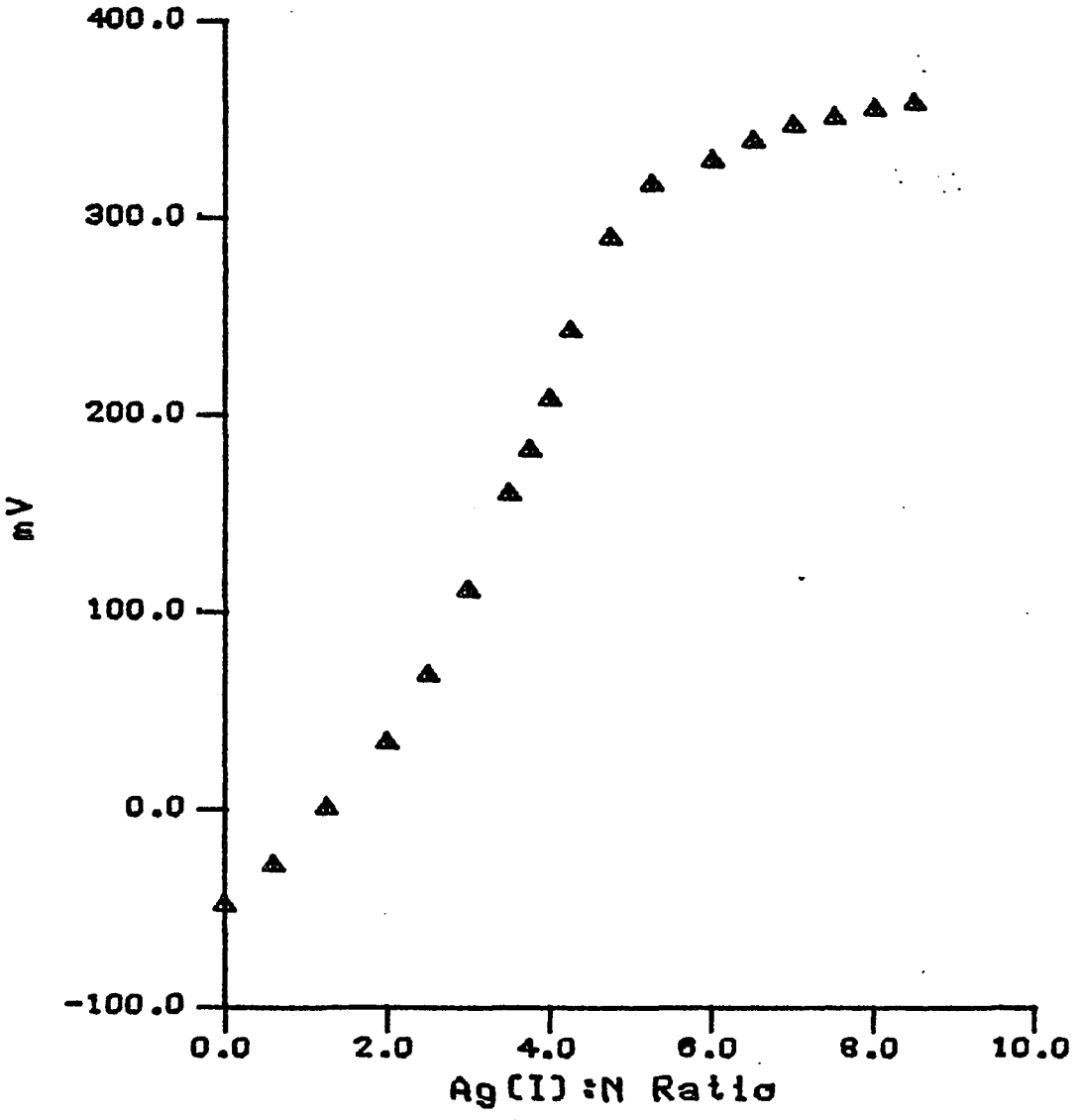

Figure 3. Potentiometric titration of PEI with 10 mM Ag(I).

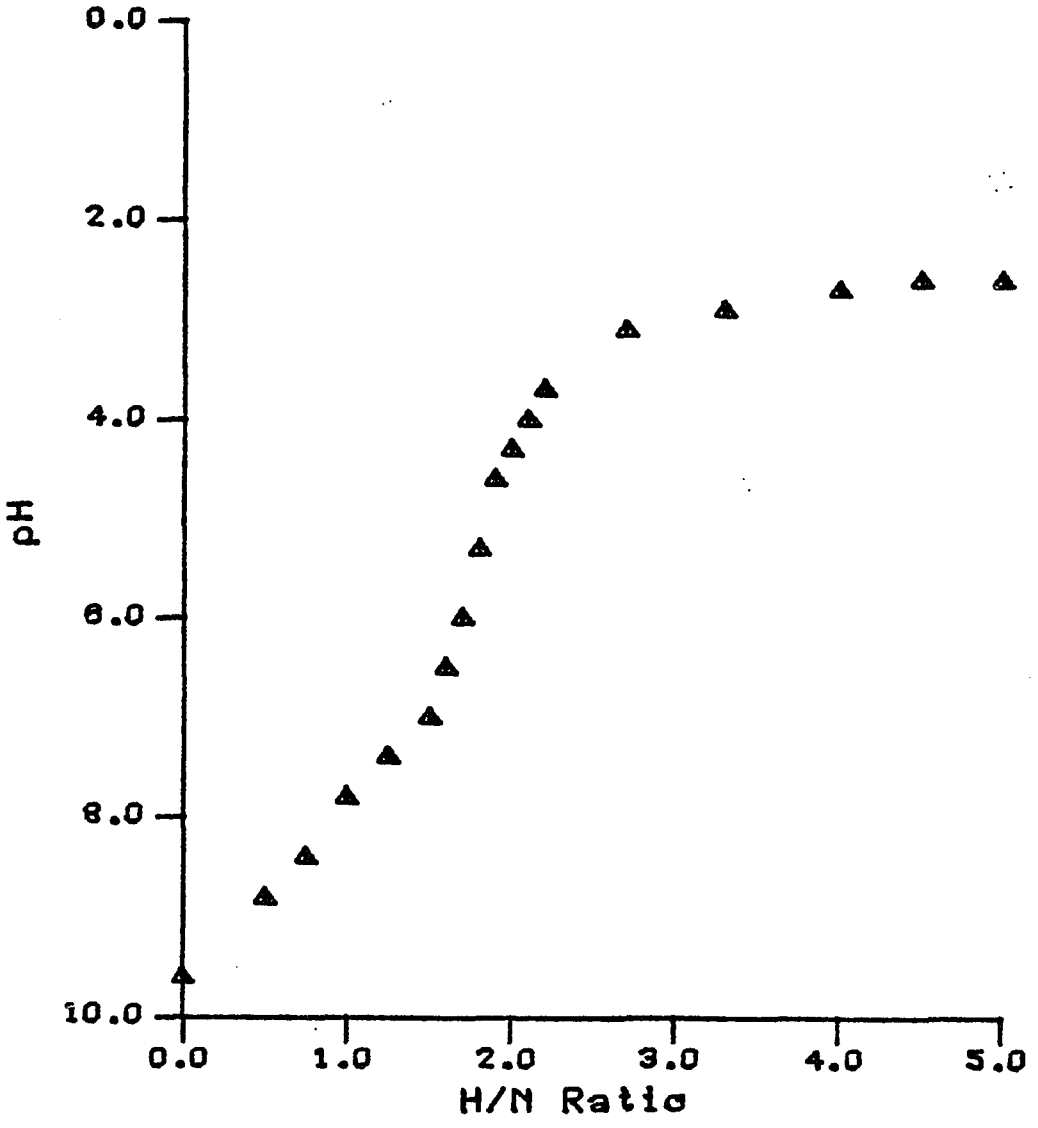

Figure 4. Potentiometric titration of PEI with 10 mM HCl.

Spectra

Fluorescence excitation and emission spectra for mono- (PySA) and tetra- (PySA4) sulfonated pyrene are shown in Figures 5 and 6, respectively. When zinc was added to the PySA system, a broad excimer peak at 470nm was also observed, as shown in Figure 7. When 363nm excitation was used (Figure 8), the emission was exclusively from excimer.

Fluorescence Titrations

Monomer vs. polymer. The effect of Cu(II) on fluorscence intensity of solutions containing PySA and either PEI or model ligand tetraethylenepentamine (tetraen) is presented in Figure 9 . Quenching efficiency for the polymeric complex shows that PySA is being bound to cationic Cu(II) sites on the polymer. In the presence of tetraen, which simulates the Cu(II) binding site on PEI, PySA fluorescence is quenched only slightly. Since the electrostatic interaction of Cu(II)-tetraen and CU(II)-PEI complexes with PySA should be similar, this observation implies that the lipophilic interaction of pyrene with the polymer backbone contributes significantly to PySA binding. This specificity also establishes that observed quenching occurs only for bound counterion rather than occurring through association in solution.

Cu(II)-PEI. The titration curves obtained for Cu-PEI, shown in Figure 10a, demonstrate the difference in binding for the two anions. Although endpoints estimated by extrapolating the straight line regions of the curve are subject to considerable uncertainty, they clearly indicate that metal:fluorophor stoichiometry is not based on

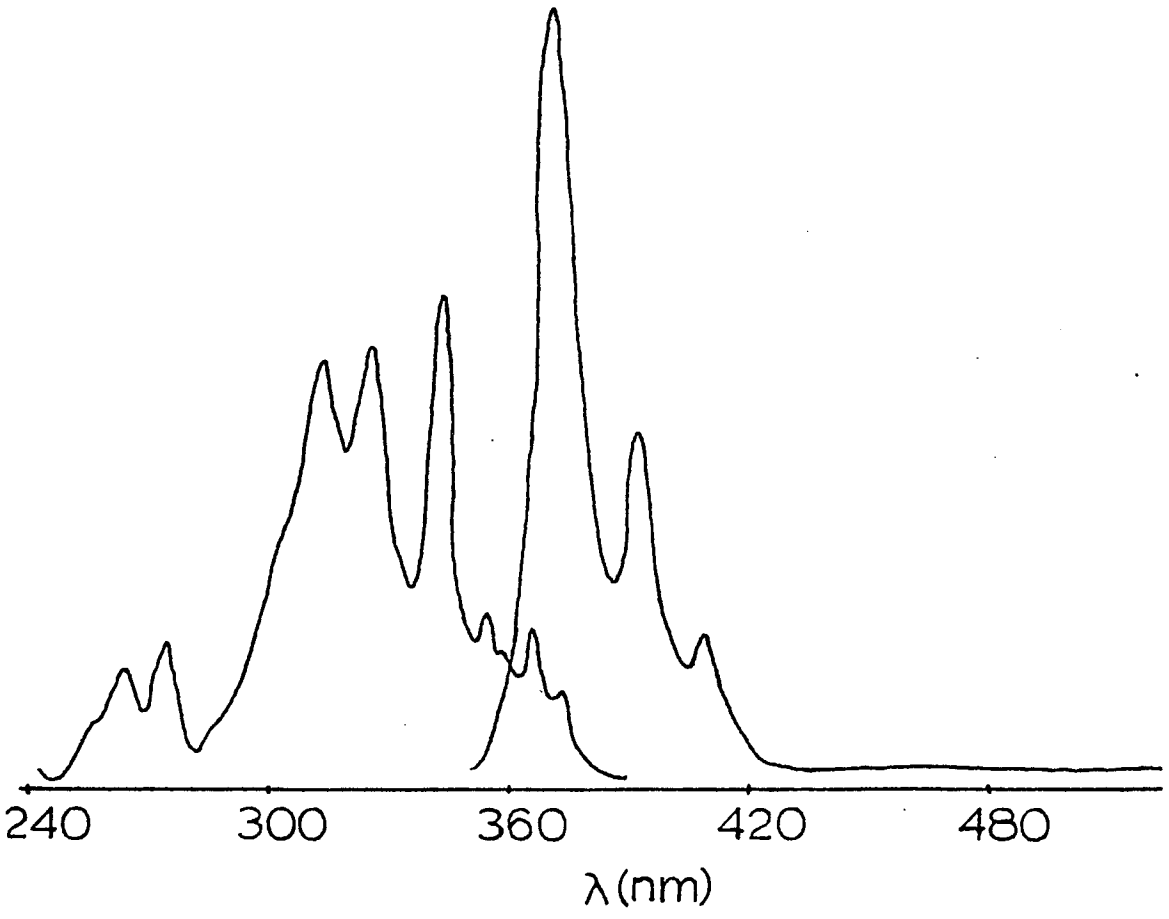

Figure 5. Excitation and emission spectra of pyrene sulfonate. Maximum emission: 374 nm; maximum excitation: 345 nm

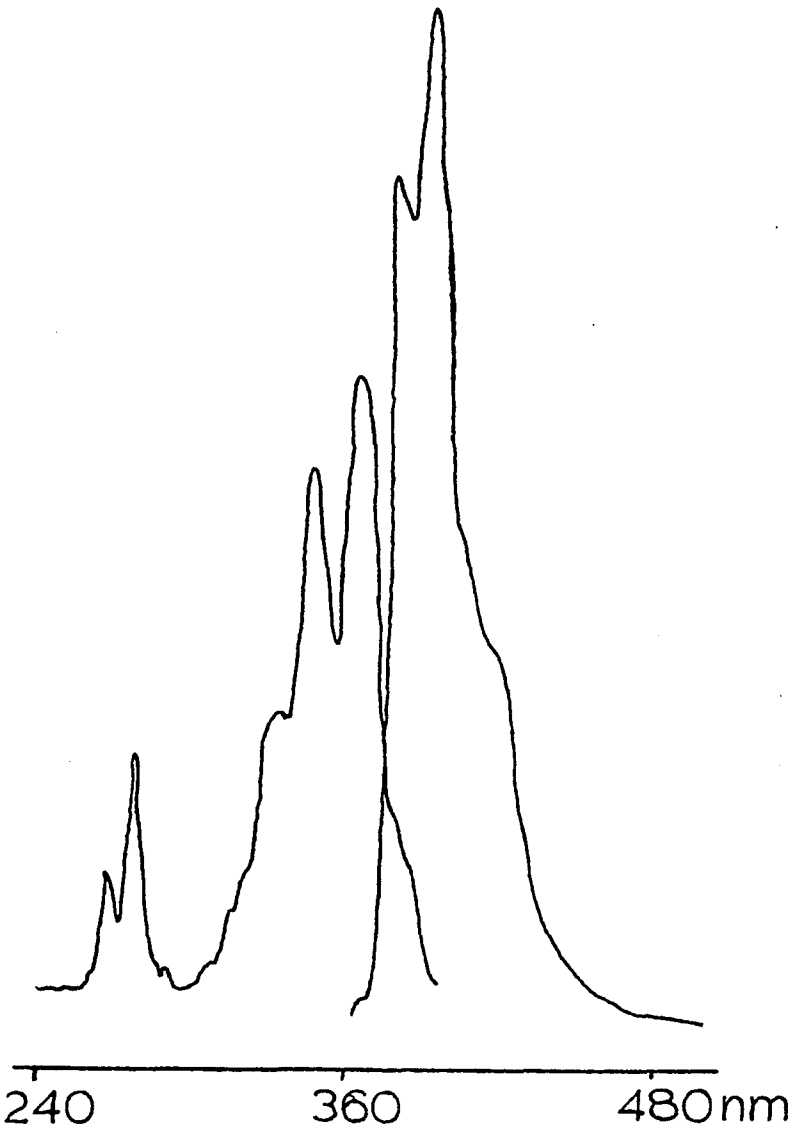

Figure 6. Excitation and emission spectra of pyrene tetrasulfonate. Maximum emission: 403 nm; maximum excitation: 368 nm

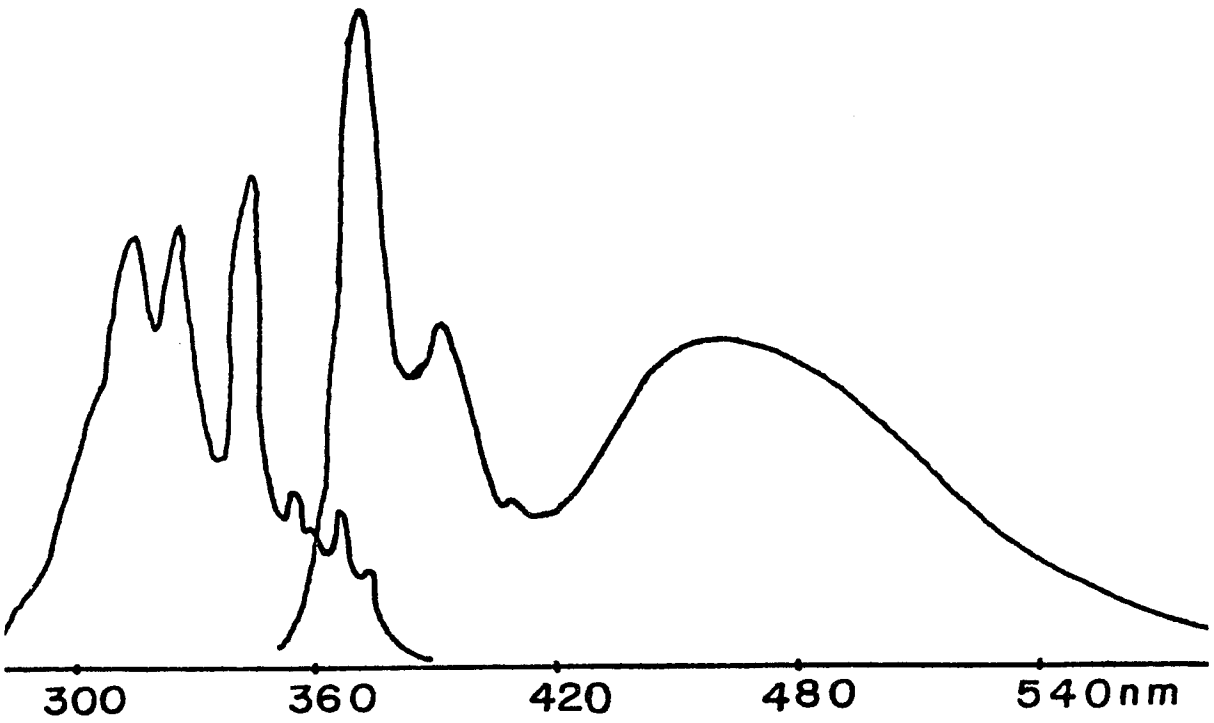

Figure 7. Pyrene sulfonate monomer and excimer emission at 470nm.

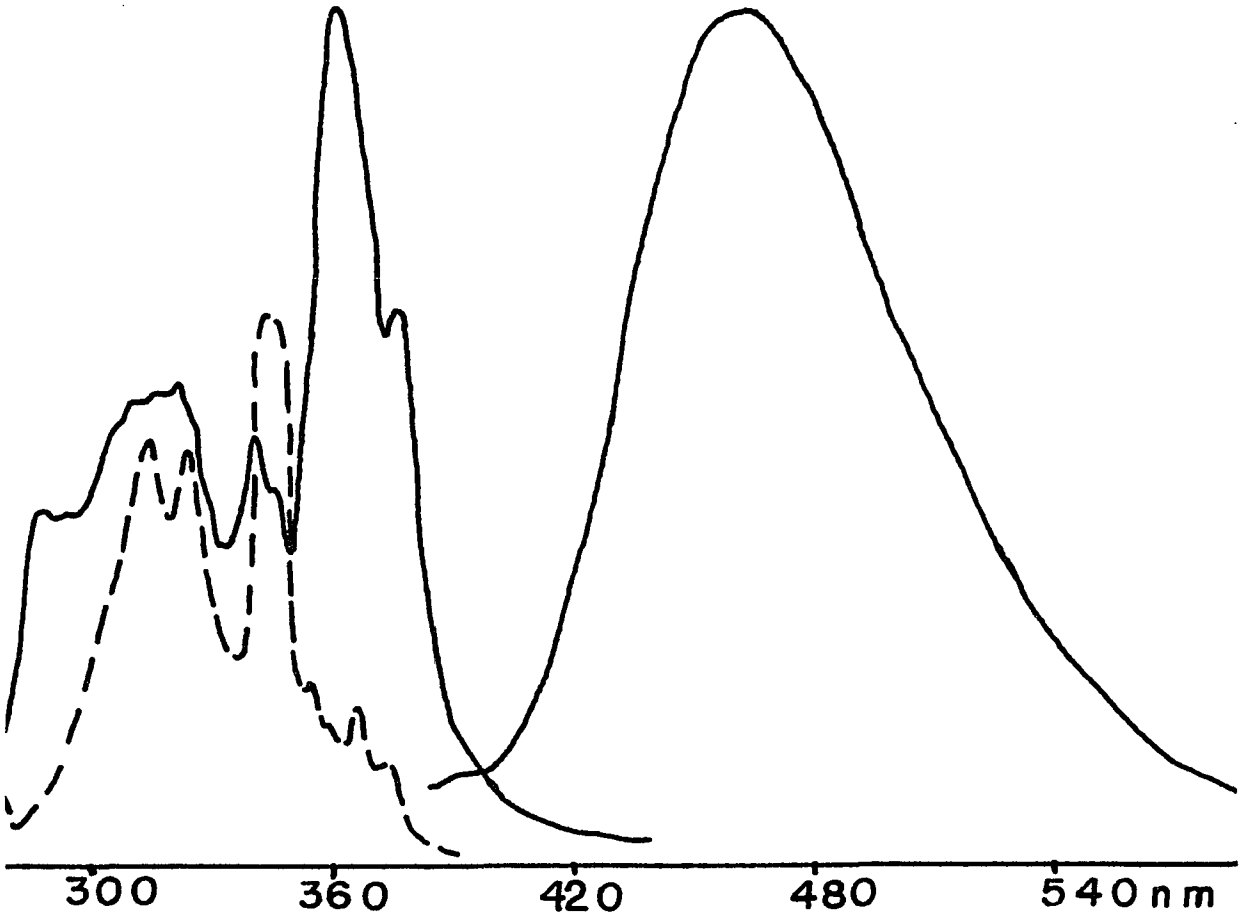

Figure 8. Pyrene sulfonate excimer emission spectrum.
Excimer emission only: Solid line excitation spectrum,
maximum = 363 nm. Dashed line: unperturbed excitation

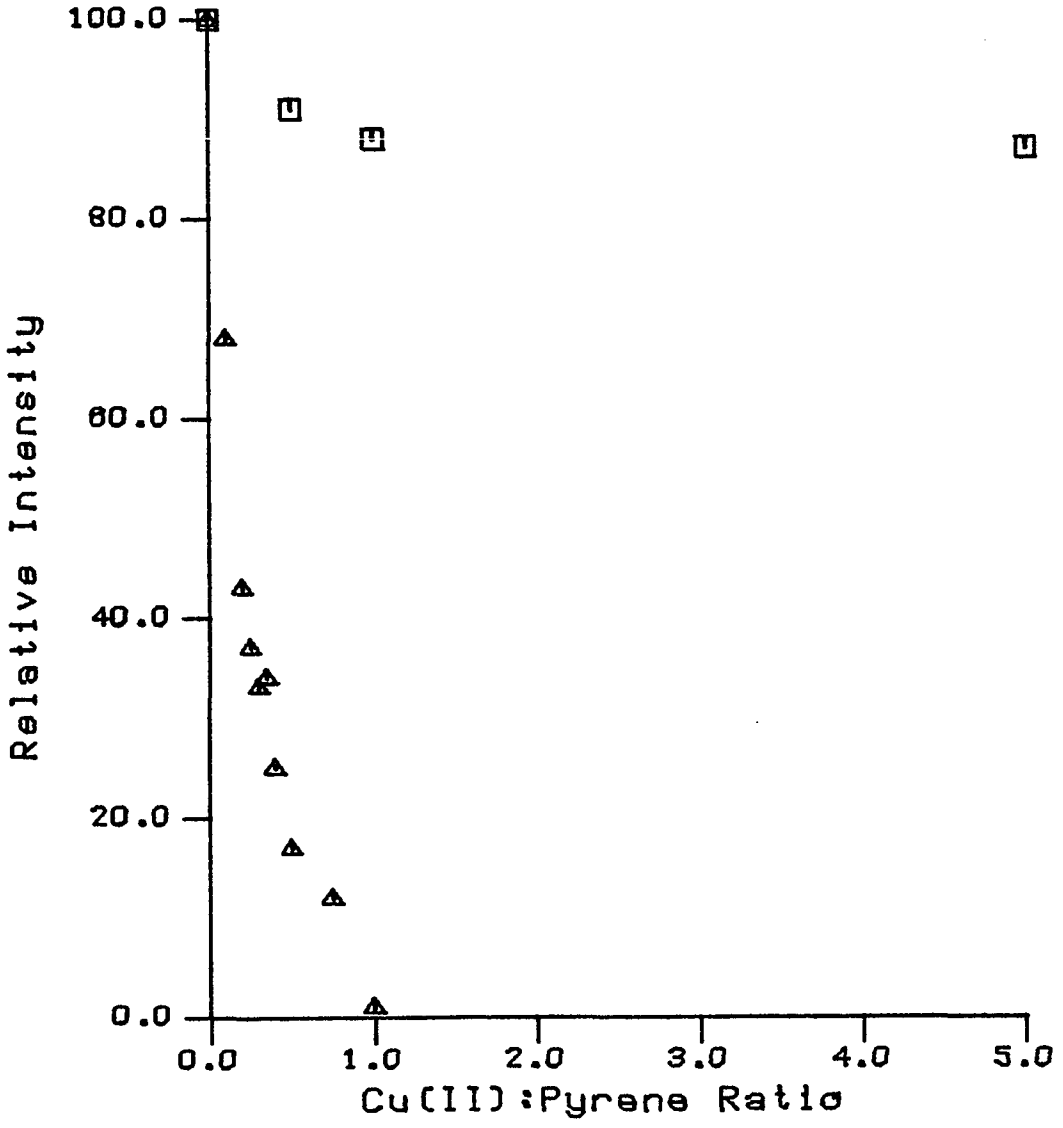

Figure 9. Fluorescence titration of model ligand (tetraen, ▯) and PEI(△) with Cu(II).

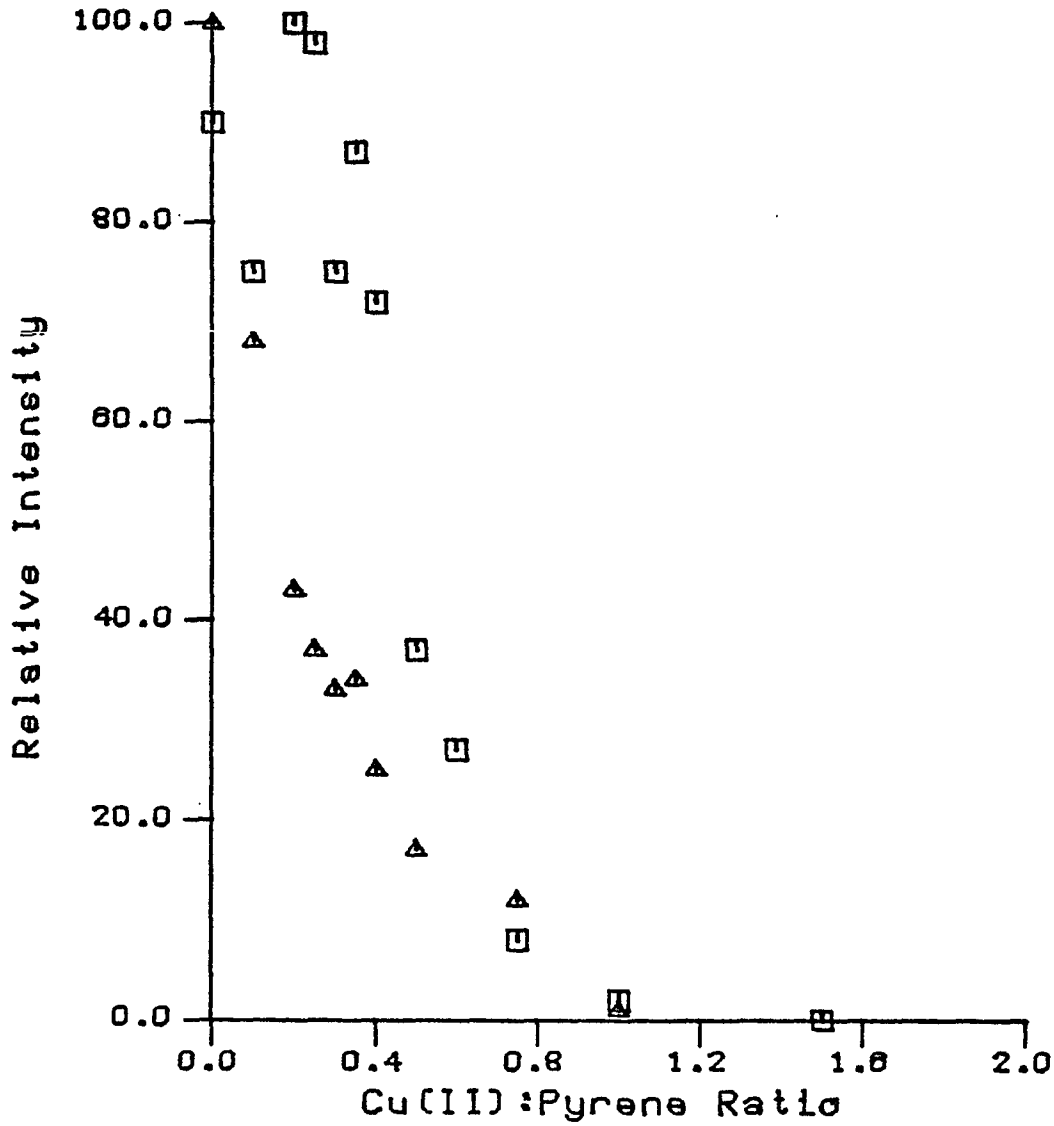

Figure 10a. Fluorescence titration of PySA (△) and PySA4 (□) with Cu(II) in the presence of excess PEI.

charge neutrality. If electrostatic interaction was the dominant binding force the endpoint ratio would correspond to neutrality: 0.5 for PySA and 2.0 for PySA4, which is not the case.

At the point in the titration curve corresponding to 0.35 Cu(II) per PySA approximately three PySA probes associate with each Cu(II) site. This indicates that strong lipophilic interactions must cause clustering of the probe molecules, leading to a PEI-Cu(II)-PySA complex with a net negative charge. Absorption spectra for the Cu(II)-PEI-PySA complexes (Figure 10b) are different before and after the endpoint. The distortion is consistent with dimer formation. As results with Zn(II)-PEI suggest (see below) PySA molecules are probably associated with each other forming ground state dimers. The pi-pi interactions between the pyrenes contribute to the overall stability of the PEI-Cu(II)-PySA system.

There is an even greater excess of negative charge in the Cu-PEI system with PySA4 as the counterion. Initially, the PySA4 curve in in Figure 10a follows the PySA curve very closely, but then the fluorescence intensity recovers and re-attains maximum intensity. The reason for this is unknown. As the Cu(II):Py ratio exceeds 0.3 there is a rapid increase in PySA4 binding. At this point, adjacent Cu(II) sites on PEI may start to get close enough together so that PySA4 can interact with two adjacent sites. Steric considerations make it unlikely that two sulfonates on a single PySA4 can interact with the same site. Charge balance considerations indicate that 1.4 sulfonates are neutralized at the endpoint in the titration curve (corresponding to 0.75 Cu(II) per PySA4), confirming that more than

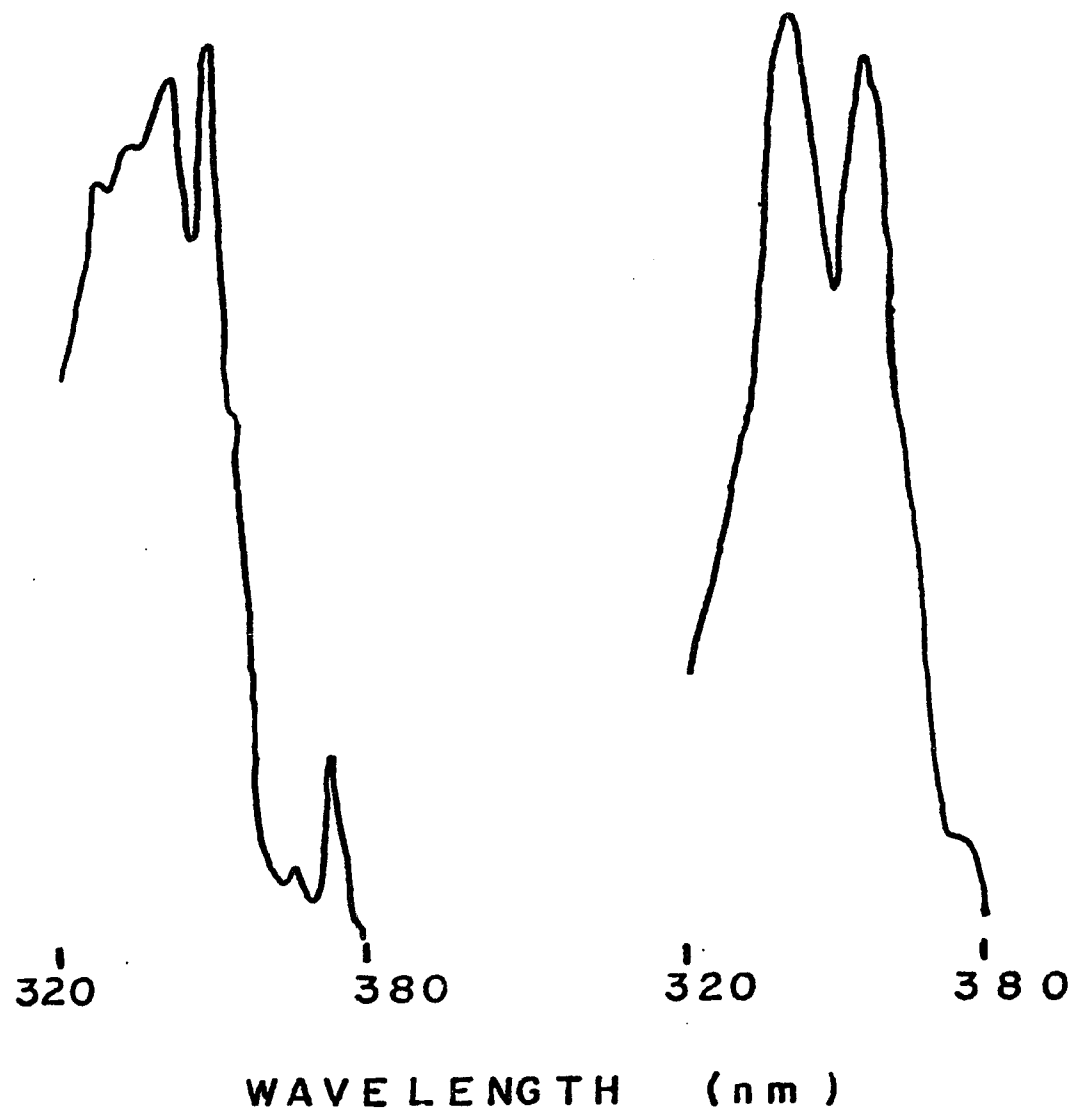

Figure 10b. Absorbance spectra of PySA-Cu(II)-PEI complexes.
Spectrum on the left shows only monomer at Cu:Py = 0.15
Spectrum on the right shows dimer forms at Cu:Py = 0.40

one sulfonate is associating with the Cu(II)-PEI site.

Zn(II)-PEI. The charge balance for Zn(II) should be the same as for Cu(II) since both are bivalent. For PySA, the titration curve in Figure 11 shows that with increasing Zn(II), monomer emission decreases and excimer emission increases. The excitation spectrum also changes (Figure 8) indicating that this is a ground state interaction. The emission peaks have completely converted to dimer at a Zn:PySA ratio of 0.4. As in the Cu(II) system, this corresponds to a net negative charge and shows the strong lipophilic driving force causing PySA to associate with polymer. The fact that ground state dimers are observed indicates that there is sufficient flexibility in the polymer to allow dimers to form without disrupting the electrostatic attraction between positive polyelectrolyte and negative counterion.

No excimer was observed with PySA4, no matter how much Zn was added, emphasizing that the presence of Zn(II) does not itself quench or alter the fluorescence of pyrene. Therefore, changes observed for PySA can be attributed to the proximity of binding. The bulky sulfonate groups may prohibit approach of neighboring PySA4 probes within excimer-forming distance.

Ag(I)-PEI. The addition of Ag(I) quenches pyrene sulfonate fluorescence as expected (Figure 12). This apparent quenching presumably reflects an increase in the rate of intersystem crossing due to the "heavy atom effect" of Ag(I). The most surprising aspect of this data is that PySA4 seems to bind more strongly than PySA. Unlike the Cu(II)-PEI system, there is not a threshold metal ion

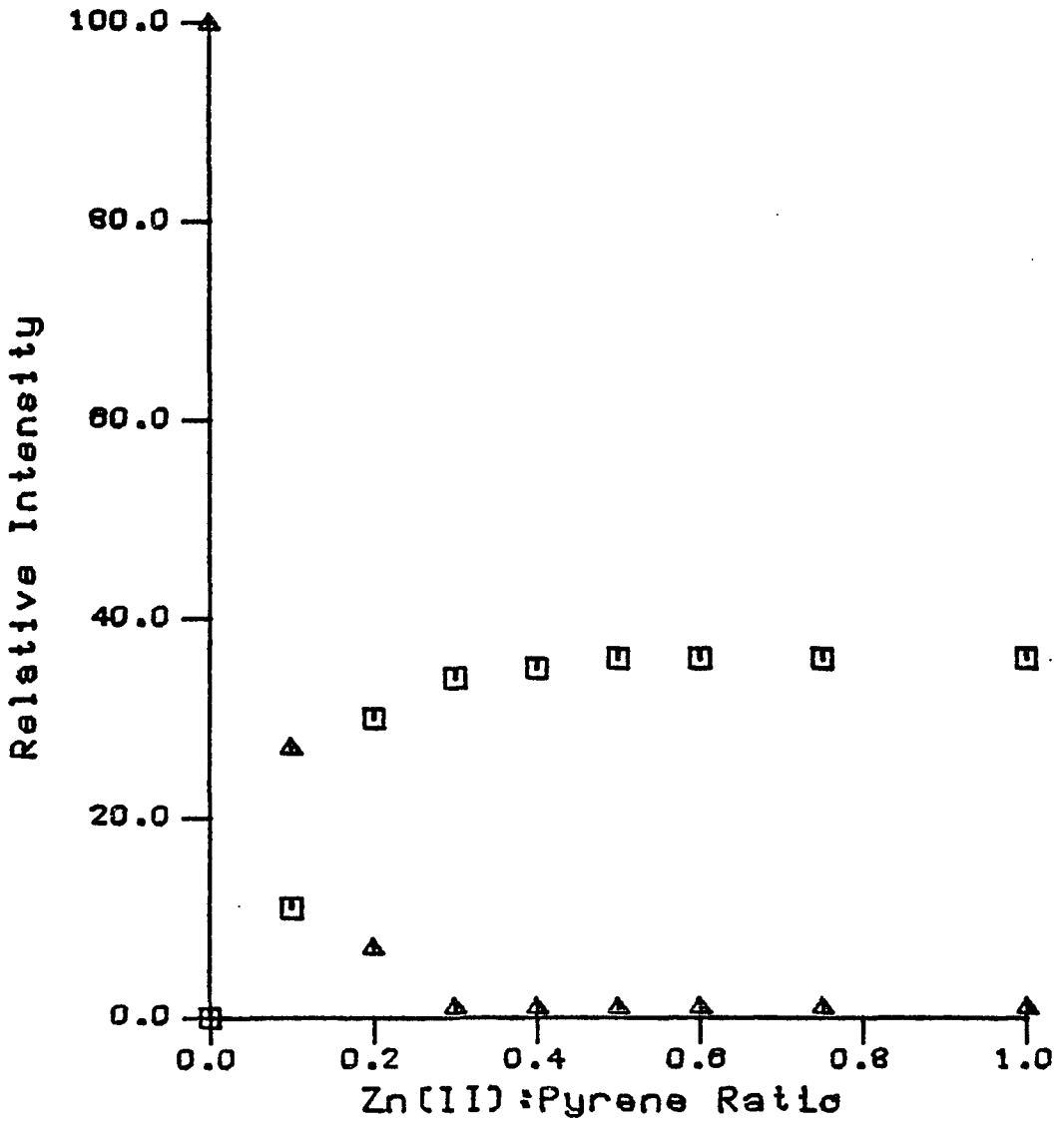

Figure 11. Fluorescence titration of PySA with Zn(II) in the presence of excess PEI.
Monomer (△) and excimer (□) emission versus Zn:PySA ratio

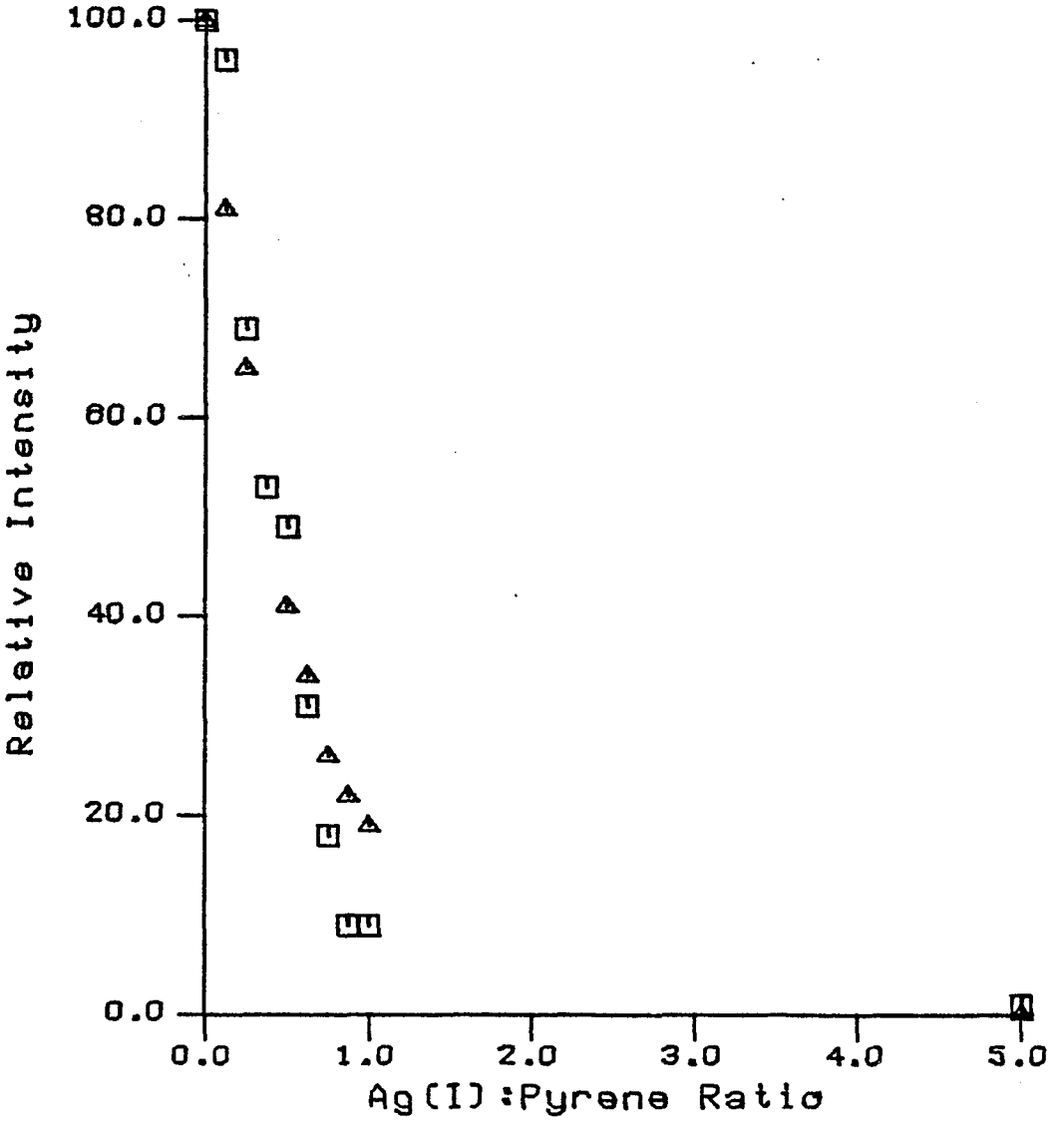

Figure 12. Fluorescence titration of PySA (▲) and PySA4 (▣) with Ag(I) in the presence of excess PEI.

level that must be exceeded to promote binding. The strong binding implies that the electrostatic interaction between sulfonate groups and the metal center is stronger in the Ag(I) system despite the lower charge on Ag(I). Since Cu(II) coordinates more monomer units than Ag(I), its charge must be more effectively screened from the sulfonate, resulting in weaker electrostatic interaction. Another way of viewing this is that the binding at the Cu(II) center is more "territorial", i.e. the PySA is not bound to a specific location. Compared to Cu(II), anion binding to Ag(I)-PEI is more "site-specific" because charge associated with the metal ion is more accessible. In general, although electrostatic forces are necessary to initiate polyelectrolyte-counterion binding, either territorial binding (structurally "loose") or site binding (stoichiometric; structurally specific) will be promoted to the extent that lipophilic interactions contribute (Turro,1983).

The potential for Ag(I)-PEI to induce phosphorescence was not realized for either PySA or PySA4 in deaerated solutions. No emission was observed in the 600nm region where phosphorescence is expected. Up to 10% of the monomer emission intensity was converted to excimer emission for PySA, however. The excimer intensity was nearly constant for all ratios of Ag(I). Excimer formation may compete with phosphorescence by promoting nonradiative triplet state-ground state interactions instead of triplet to ground state decay via phosphorescent emission (Thomas). The fact that less excimer is formed with Ag(I) than with Zn(II) could depend on charge. It could also reflect the fact that the more site-specific binding by

Ag(I) makes it more difficult for adjacent PySA probes to achieve a configuration favoring ground state dimer formation.

Proton-PEI. Saturation of PEI with protons did not affect luminescence behavior. Emission from pyrene in PEI solutions was unchanged until metals were introduced into the system. The importance of a metal center to induce these effects is clear. Altered excited state behavior results from more than net charge alone since the polymer saturated with protons shows nearly constant monomer emission intensity and no excimer emission at all, unlike the polymer saturated with monovalent metal ion. This comparison provides infomation about the greater ability of the metal to define a territorial environment. Counterions apparently associate with specific sites on protonated PEI, in which each proton binds to a single monomer unit. This supports the conclusion that as more ligands surround a cationic center, electrostatic interactions become weaker and lipophilic interactions stronger, resulting in binding that is more territorial in nature. If a territorial environment was created by the native polymer backbone, the pyrene proximity would favor excimer emission.

Conclusions

This study yields information on the microenvironment of anionic fluorophors immobilized at a metal center site on polyethylenimine. The organic anion is attracted to the metal centered site where it is bound by a combination of electrostatic and lipophilic interactions. The extent of interaction depends on the density of charge around the metal center, which is a function of the strength and coordination of metal-PEI chelation. The stoichiometry of counterion binding to metal

centers is not consistent with electroneutrality, indicating that lipophilic interactions are important. Excimer emission from ground state dimers is indicative of site proximity and cluster formation.

It is possible to manipulate the relative contributions of electrostatic and lipophilic interactions in order to immobilize anionic reagents in a predictable and useful manner. This can be accomplished by proper choice of metal center and anion to influence the extent of site binding to the metal center versus territorial binding within the the polymer backbone. The formation of clusters can provide the proximity and microenvironment suitable for analyses requiring altered luminescence behavior.

CHAPTER IV

INTRAMOLECULAR ENERGY TRANSFER

Introduction

This chapter deals with fluorescence depolarization due to intramolecular energy transfer between two or more equivalent fluorophors. When one fluorophor is excited, it can transfer its energy to the other fluorophor(s) within the molecule, providing certain conditions are satisfied. This process randomizes the orientation of the transition moments involved in emission, thus causing a decrease in the polarization of fluorescence.

Intramolecular energy transfer can be used to detect changes in structure or differences between complexes with otherwise identical spectral characteristics because the efficiency of energy transfer depends on the number of fluorophors and their relative orientation. Analytically, this phenomenon can be exploited to distinguish molecules or complexes containing single fluorophors from species containing multiple equivalent fluorophors.

The systems studied were crown ethers, metal complexes, and organic bifluorophors. In the crown ether system energy transfer enabled us to look at the change in angle between two equivalent fluorophors on the cyclic polyether. Complexation of alkali metal ions to crown ethers provides a highly sensitive and selective

fluorimetric method for determination of those ions. The crown ether reagents and complexes have identical spectra, so the analysis normally involves a separation. The separation can be avoided by detecting polarization differences.

The metal complexes studied were those in which the ligands fluoresce only when bound to metals. These ligands are commonly used for determination of metal ions. Although binding is generally nonspecific, the number of ligands in the complexes will be a function of the coordinative saturation of the metal. Intramolecular energy transfer is only observed for those ligands bound to a common metal center. Thus it is possible to differentiate complexes on the basis of stoichiometry. The organic bifluorophor studied demonstrates the potential of this technique to determine an average angle between equivalent fluorophor groups on a single molecule in solution.

Background

Fluorescence Polarization

The theory of fluorescence polarization is presented by WEBER (Hercules). The molecule is excited with plane polarized light. Emission is resolved by polarizers into components parallel and perpendicular to the excitation radiation, Iii and I⊥, respectively. The polarization, p, is calculated from these intensities.

$$p = (I_{ii} - I_{i\perp})/(I_{ii} + I_{i\perp}) \quad (1)$$

The intrinsic polarization, Po, is the maximum value for any fluorophor. It reflects the orientation of the transition moment for the excitation process relative to the transition moment for emission in

the absence of depolarizing processes.

Fluorescence can be depolarized in solution by rotation of the fluorophor during the lifetime of the excited state or by energy transfer. Rotational depolarization is effectively eliminated in this work by the use of a high viscosity solvent, glycerol. Depolarization is also observed when fluorophors are sufficiently close together for a significant degree of intermolecular energy transfer to occur. This process is designated concentration depolarization; as such it is not important in this work since concentrations are sufficiently low. Thus, all depolarization observed can be attributed to the intramolecular process of interest.

For any depolarizing process the observed polarization, p, depends on the intrinsic polarization, Po, and $\overline{\cos^2 w}$, the average of the square of the cosine of the angle(s) of extrinsic depolarization, i.e. the angle over which the fluorescent moment changes due to the depolarizing process.

$$(1/Po - 1/3) = (1/P - 1/3)(2/3\ \overline{\cos^2 w} - 1) \qquad (2)$$

If a molecule does not change its orientation between excitation and emission, Po is observed. The difference in orientation applies only to excited molecules; not to the molecular population as a whole, which remains randomly oriented at all times.

Absorption of excitation radiation is at a maximum for fluorophors whose transition moment is parallel to the incident radiation. If excitation energy migrates from an absorbing fluorophor to another equivalent fluorophor on the same structure, the emitting fluorophor will be at a different orientation from the absorbing fluorophor; and

result in a decrease of fluorescence polarization.

Structure-Polarization Relationship

In principle, measurements of polarization should provide information on the structure of compounds containing multiple fluorophors, Fn. For a compound, A, of composition AFn,

$$\overline{\cos^2 w} = (1/n)(\cos^2 0 + (n-1)\cos^2 z) \qquad (3)$$

where z is the angle between emission transition moments associated with individual fluorophors on the same molecule and w is the angle of extrinsic depolarization. This equation assumes that energy is equally distributed among the equivalent fluorophors.

The rate of energy transfer can be estimated from the critical radius for Forster energy transfer. Values can be calculated using lifetime data and experimental parameters. However, the addition of successive fluorophors to a compound may perturb the electronic properties of equivalent fluorophors in such a manner as to alter the polarization in a nonquantitative way. Perturbations of this sort can be detected by spectral shifts and divergent polarization spectra. Structural distortions could also limit the quantitative information obtained from this method. In particular, a solvent that binds to the fluorophor(s) or to any other portion of the compound of interest could alter the structure.

Energy Transfer

For fluorescence to be depolarized by intramolecular energy transfer, conditions must be favorable for energy transfer from one fluorophor to the other. If energy transfer is rapid relative to fluorescence, the excitation energy will be randomly distributed

among all fluorophors prior to emission. The theoretical basis for non-radiative transfer of excitation energy was developed by FORSTER, and is commonly referred to as Forster energy transfer. The molecules must be within a critical radius, properly oriented, and the absorbance and fluorescence peaks must overlap to some extent. The rate of energy transfer, kT, and the efficiency, E, are defined by Forster as:

$$kT = r^{-6}K^2Jn^{-4}kF \times 8.71 \times 10^{23}\ sec^{-1} \quad (4)$$

$$E = r^{-6}/(r^{-6} + Ro^{-6}) \quad (5)$$

The critical radius, Ro, can be calculated (Stryer):

$$Ro = 9700\text{Å}(JK^2Q_on^{-4})^{-6} \quad (6)$$

Ro is the distance at which energy transfer and emission without transfer are equally likely. The geometric variables are (1) r: the distance between the donor and acceptor, on which there is an inverse sixth order dependence and (2) K: the orientation factor (usually considered to be an average value, 2/3 when dealing with solutions). The spectroscopic variables are (1) J: the spectral overlap integral (for the energy of the acceptor fluorophor excitation and donor fluorophor emission peaks); (2) n, the refractive index of the solvent; (3) kF, the rate constant for fluorescence (the reciprocal of the lifetime); and (4) Qo, the quantum yield of fluorescence efficiency for the donor fluorophor. In this study the donor and acceptor are equivalent fluorophors. For small molecules in viscous solution, Ro ranges from 15-40 Å. Any Ro calculated to be within or below this range indicates conditions for efficient, rapid energy

transfer are met.

Crown Ethers (Structures, Figure 1a)

The ring radius of a typical cyclic polyether is very similar to the ionic radii of alkali metals, on the order of 2Å (Pedersen). As a result, equivalent fluorophors attached to the same ring will be well within the critical radius for energy transfer. Although the spectral overlap is poor for equivalent fluorophors, energy transfer is still rapid in view of the inverse sixth order dependence on distance. The orientation factor, K, depends on the angle between the fluorophors. However, even if it is unfavorable, energy transfer should be rapid due to the distance factor.

The conformation of dibenzo-18-crown-6 (DB18C6) is known to differ for the free and complexed forms. The complex structure is planar or semiplanar both in ground and excited states (Shizuka). The complex conformation in solution has been proposed (Live) to be the same as the crystal structure (Bush), whereas the solution conformation of the free DB18C6 differs from the crystal structure. The structures proposed (Live) are shown in Figure 1b. The crown ether ring flattens upon complexation, thereby increasing the angle between fluorophors bound to the ring (Shizuka). There is a corresponding increase in the angle between fluorescent transition moments, which are perpendicular to the plane of the ring. The increase in angle is most pronounced for the potassium complex, which is attributed to the fact that the radius of the cavity of 18C6 (1.3-1.6Å) matches the ionic radius of potassium (1.49Å). Similar effects are observed for Li, Na, Rb, and Cs to a lesser extent. Thus, the system chosen for

a.

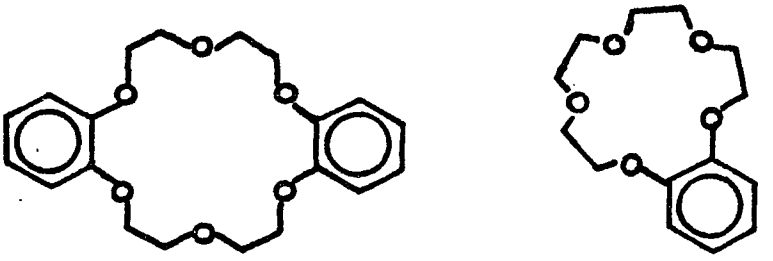

DB18C6 B15C5

b.

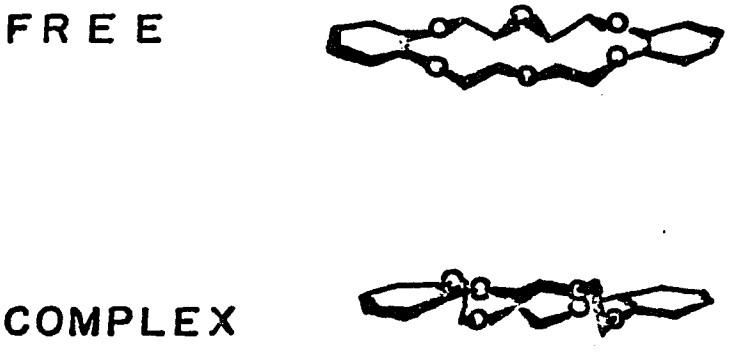

Figure 1. Structures of crown ether compounds.
a. compounds used b. conformation of DB18C6 and DB18C6-K

study was DB18C6-K.

Metal-Ligand Complexes (Structures Figure 2)

In this system, the equivalent fluorophors are ligands bound to a metal center. 8-quinolinol (oxine) and morin (polyhydroxyflavone) were selected as ligands to study intramolecular energy transfer among ligands because (1) they form complexes of varying ligand/metal ratio and (2) they fluoresce efficiently only when bound to metal ions (Seitz).

8-Quinolinol. Although 8-quinolinolates of many metals are known to fluoresce, investigations of the fluorescence of these chelates have been largely confined to the development of specific analytical methods (Ohnesorge, 1959). The problem is that for a given ligand, both absorbance and emission maxima from different metal complexes are at essentially the same wavelengths (Bhatnagar). Various complexes may be distinguished on the basis of their excited state lifetimes by time-resolved spectroscopy (Lytle). However, this technique requires sophisticated instrumentation. Polarization, in contrast, can be determined with modest additions to conventional fluorescence instrumentation. It has been shown that binary mixtures of metal-oxine complexes can in some cases be resolved based on differences in the polarization of their fluorescence (Stepanova). Intramolecular, or ligand-ligand, energy transfer has been proposed as a factor affecting the polarization of complex fluorescence in the solid phase (DeArmond) although it has not previously been demonstrated in solution.

The formula of the highest complexes studied in this thesis have

a.

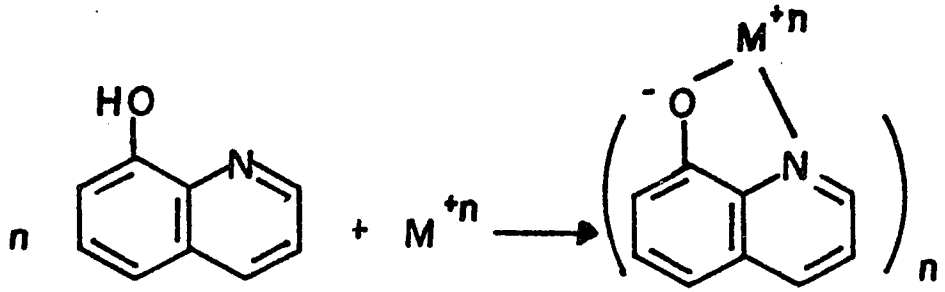

b.

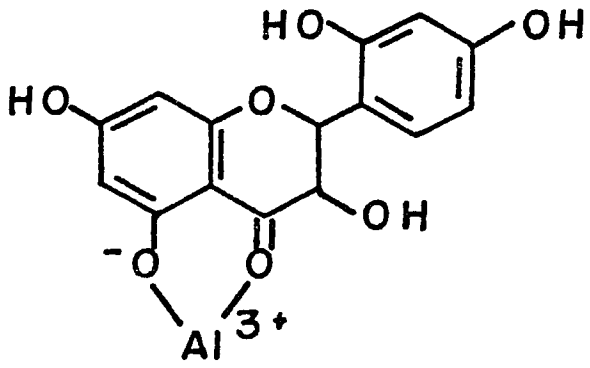

Figure 2. Structures of metal complexes studied.
a. 8-quinolinol b. morin

been shown to be $Mg(Ox)_2.2H_2O$, $Zn(Ox)_2.H_2O$, and $Al(Ox)_3$ (Lytle). The crystal structure of the hydrated zinc complex is a distorted octahedron (Merritt). Aluminum complexes are usually octahedral (Ohnesorge, 1967). Others have studied the effect of solvent (Lytle; Popovych) and electronic structure of the cation (Stevens) on fluorescence efficiency in metal quinolate complexes. Zinc complexes of the methyl derivatives of 8-quinolinol in absolute ethanol incorporate solvent as a ligand (Carter). The role of the solvent is of particular interest here since the glycerol could bind as a competing bidentate ligand.

Morin. The hydroxyflavones in general, and morin in particular, are excellent reagents for the spectrophotometric and fluorometric determination of several cations (Katyal). 2',3,4',5,7-pentahydroxyflavone (morin) is known to form 2:1 complexes with several metals (Argauer). The hydroxyl group at either position 3 or 5 and the adjacent carbonyl bind the metal. Flavones with free hydroxyls at either (or both) of these positions have been used to detect Al in several analytical procedures because they fluoresce efficiently. The structure of these complexes is probably tetrahedral (Wong).

Experimental

All fluorophors and metal salts were reagent grade or better and were used without further purification. Triethanolamine was glass distilled immediately before use. Benzo-15-crown-5 (B15C5), dibenzo-18-crown-6 (DB18C6), p-cresol, 4,4'-methylene diphenol and morin (indicator grade 2',3,4',5,7-pentahydroxyflavone) were purchased from Aldrich. 8-Quinolinol and metal salts were Baker

Analyzed Reagents. Glycerol was Aldrich Gold Label (99.8+% spectrophotometric grade) and absolute ethanol was reagent grade. All water was deionized and glass distilled.

Stock fluorophor solutions in absolute ethanol and metal salts in distilled water were diluted to volume with glycerol. Triethanolamine was added to 8-quinolinol systems to promote complexation. In all cases, glycerol comprised at least 99.5% of the solvent system.

All spectral information was obtained at room temperature (18.5-27.5°C) in glycerol. Temperature was constant (±1°C) for each fluorophor studied. Excitation and emission maxima for each system were obtained by scanning on a Perkin Elmer 204 Fluorescence Spectrophotometer. Absorption spectra were obtained on a Varian Cary 219 Spectrophotometer.

Polarization and intensity data were obtained on an SLM 8000 Photon Counting Spectrofluorometer (SLM Instruments, Inc., Urbana IL). The 450W xenon arc source radiation passes through a grating monochromator and Glan Thompson polarizer before illuminating the sample. Emission is polarized by film polarizers and detected by photomultiplier tubes. There are two detectors for simultaneous measurement of parallel and perpendicular intensities. Excitation radiation is blocked by long pass filters (Schott Optical; Corion). Maximum throughput was obtained using 8mm slits (16nm bandpass). Data acquisition for 1 second was electronically corrected for dark current background and solvent and/or excess ligand background was subtracted prior to calculating polarization. Polarization values

represent an average of five data acquisitions. The relative standard deviation of average intensity measurements was <1%, resulting in polarizations precise to ±0.001.

Results

Crown Ether System

The polarization values for DB18C6 and B15C5, free and with excess potassium are presented in Table 1a. Relative polarizations as a function of wavelength for both crown ethers were unchanged with added potassium, as shown in Table 1b.

Metal Complexes

Polarization vs. Ligand/Metal Ratio. Polarization as a function of 8-quinolinol/metal ratio for Al(III), Mg(II), and Zn(II) is presented in Figure 3. The polarizations for all three metal complexes are almost identical when the metal is in excess. Under these conditions only the 1:1 complex can form, and the observed polarization is the intrinsic polarization for ligand fluorescence. As the ligand/metal ratio increases, polarization decreases, ultimately reaching a limiting value. The limiting values are similar for Mg and Zn but lower for Al.

In Figure 4 polarization is a function of morin/Al ratio. The inability to reach a limiting value indicates that there is a mixture of 2:1 and 1:1 complex. Background fluorescence from uncomplexed morin established the maximum morin/Al ratio that could be studied.

Spectra. Polarization spectra for the 1:1 complexes (excess metal) and the limiting complexes (excess ligand) for 8-quinolinol are presented in Figure 5. The dependence of polarization on

Table 1

Polarization of Crown Ethers

a. Polarization of 10^{-5}M crown ether solutions, free and in presence of 500-fold excess potassium. λex=280nm; λem=305nm; LP filter=305nm

Crown	Polarization
Benzo-15-Crown-5	0.295
B-15-C-5 - K^+	0.295
Dibenzo-18-Crown-6	0.154
DB-18-C-6 - K^+	0.190

b. Polarization spectra of crown ethers (polarization as a function of excitation wavelength, λex)

	DB18C6 Polarization		B15C5 Polarization	
λex	Blk	K^+	Blk	K^+
265	0.088	0.108	0.172	0.172
270	0.108	0.141	0.230	0.232
275	0.135	0.168	0.274	0.272
280	0.154	0.190	0.295	0.295
285	0.167	0.212	0.315	0.312

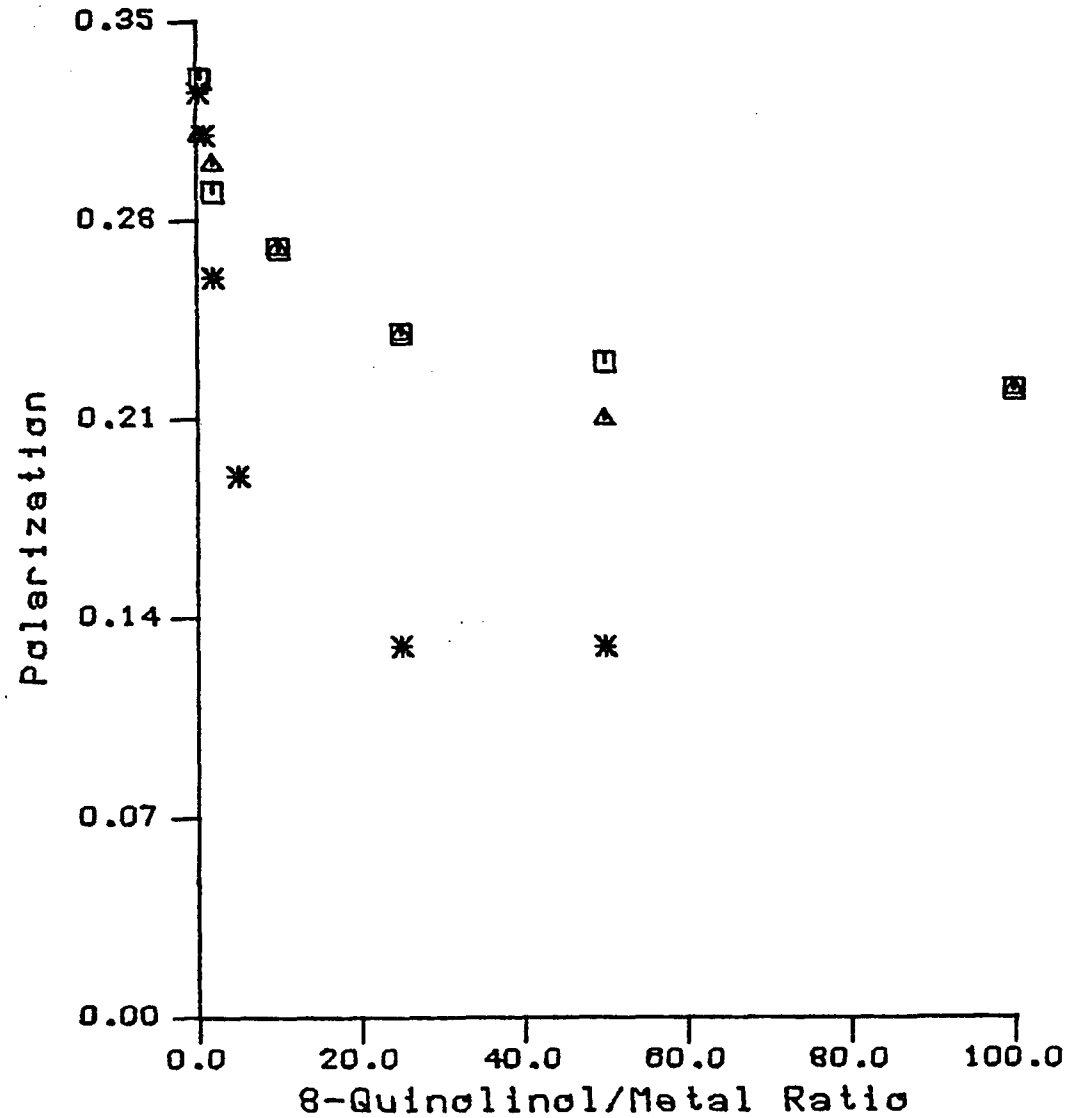

Figure 3. Polarization of 8-quinolinol fluorescence as a function of ligand/metal ratio for excitation at 370 nm; emission at 518 nm. Metal concentration 5X10 M. Al (✱), Zn(□), Mg(△)

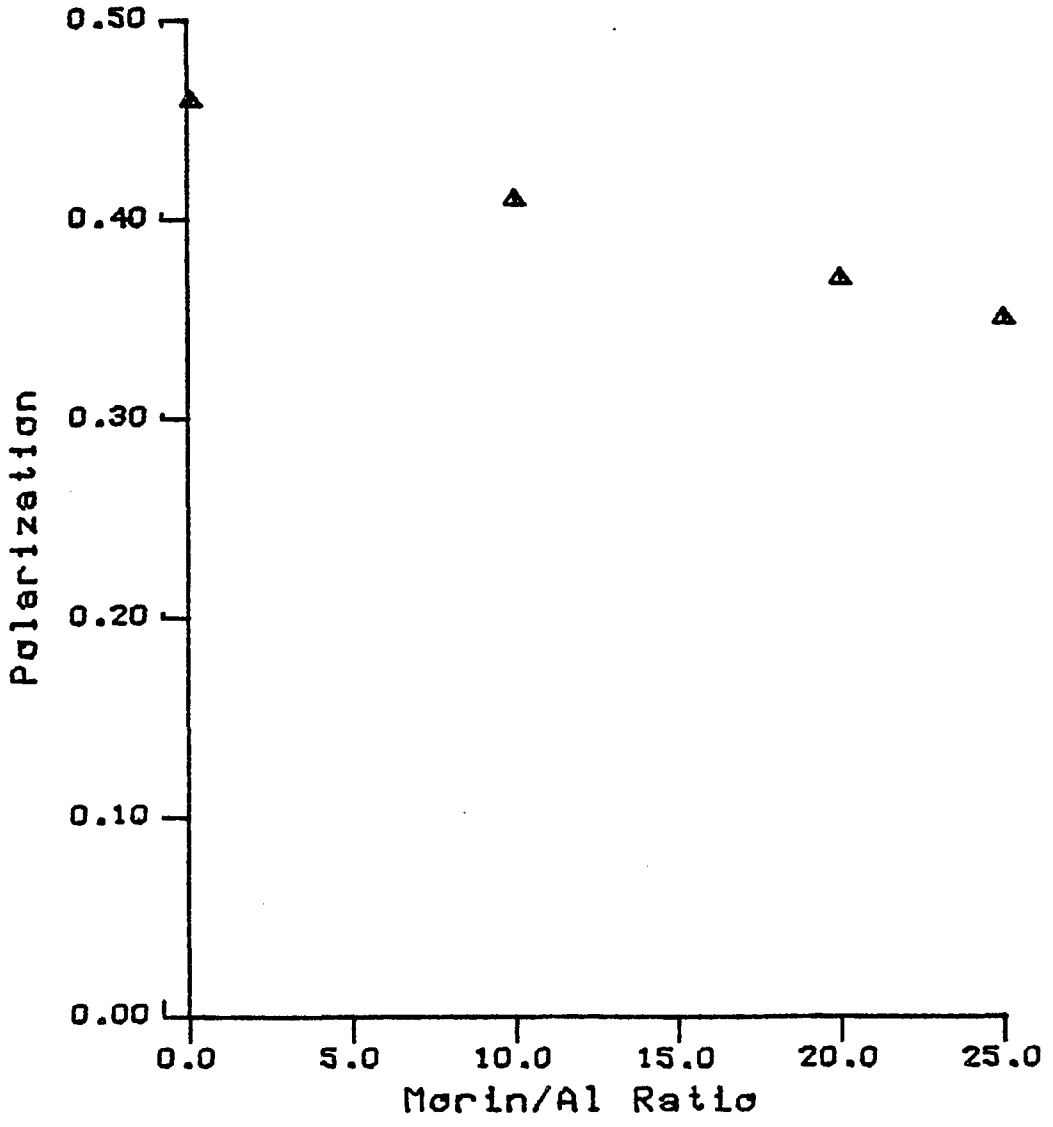

Figure 4. Polarization of morin fluorescence as a function of morin/aluminum ratio for excitation at 430 nm; emission at 493 nm.

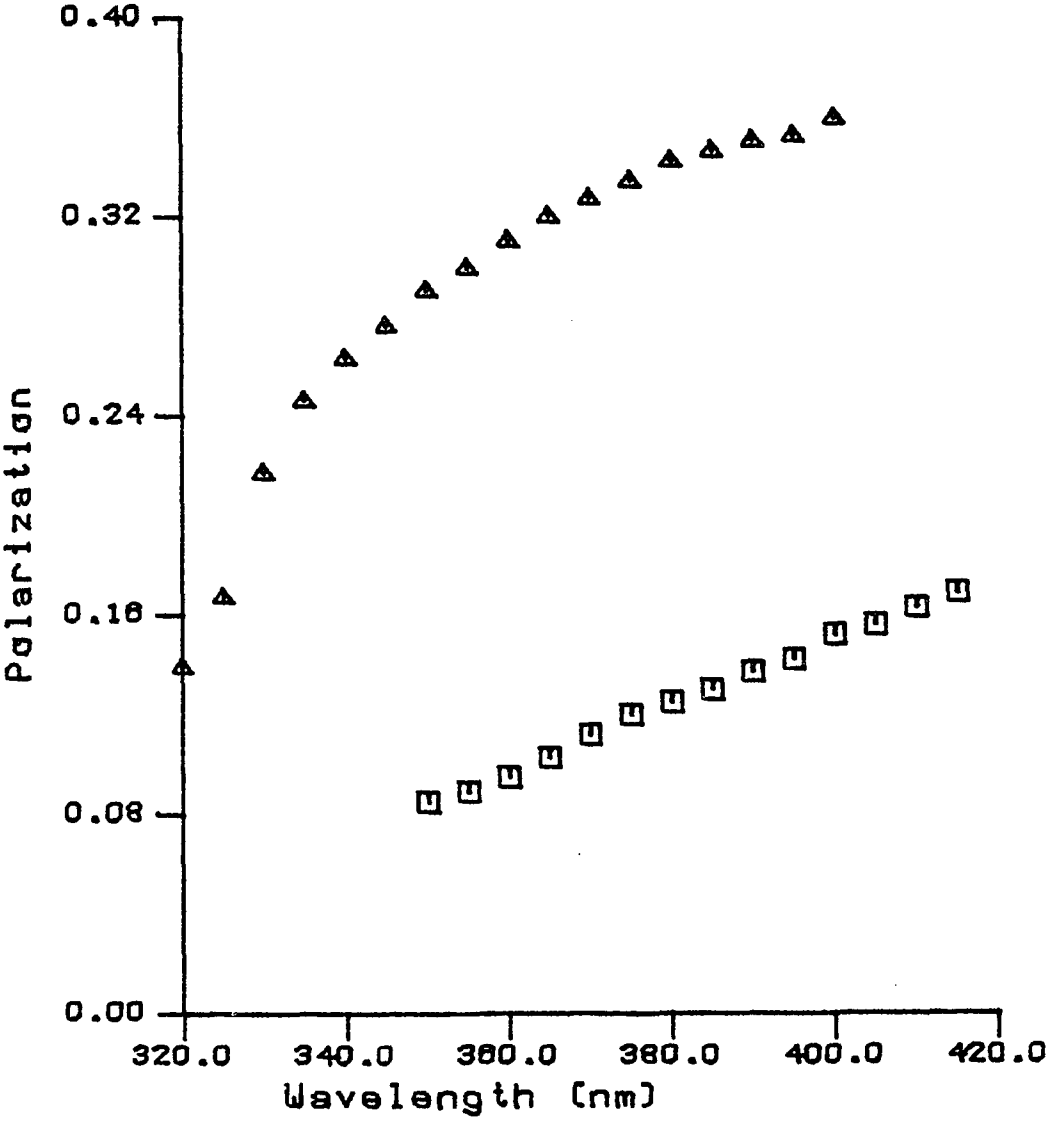

Figure 5. Polarization spectra, Al-8-quinolinol complexes. Emission through long pass filter with 50%T at 518 nm; Bandpass: 4nm. 1:1 complex (△); 3:1 complex (□)

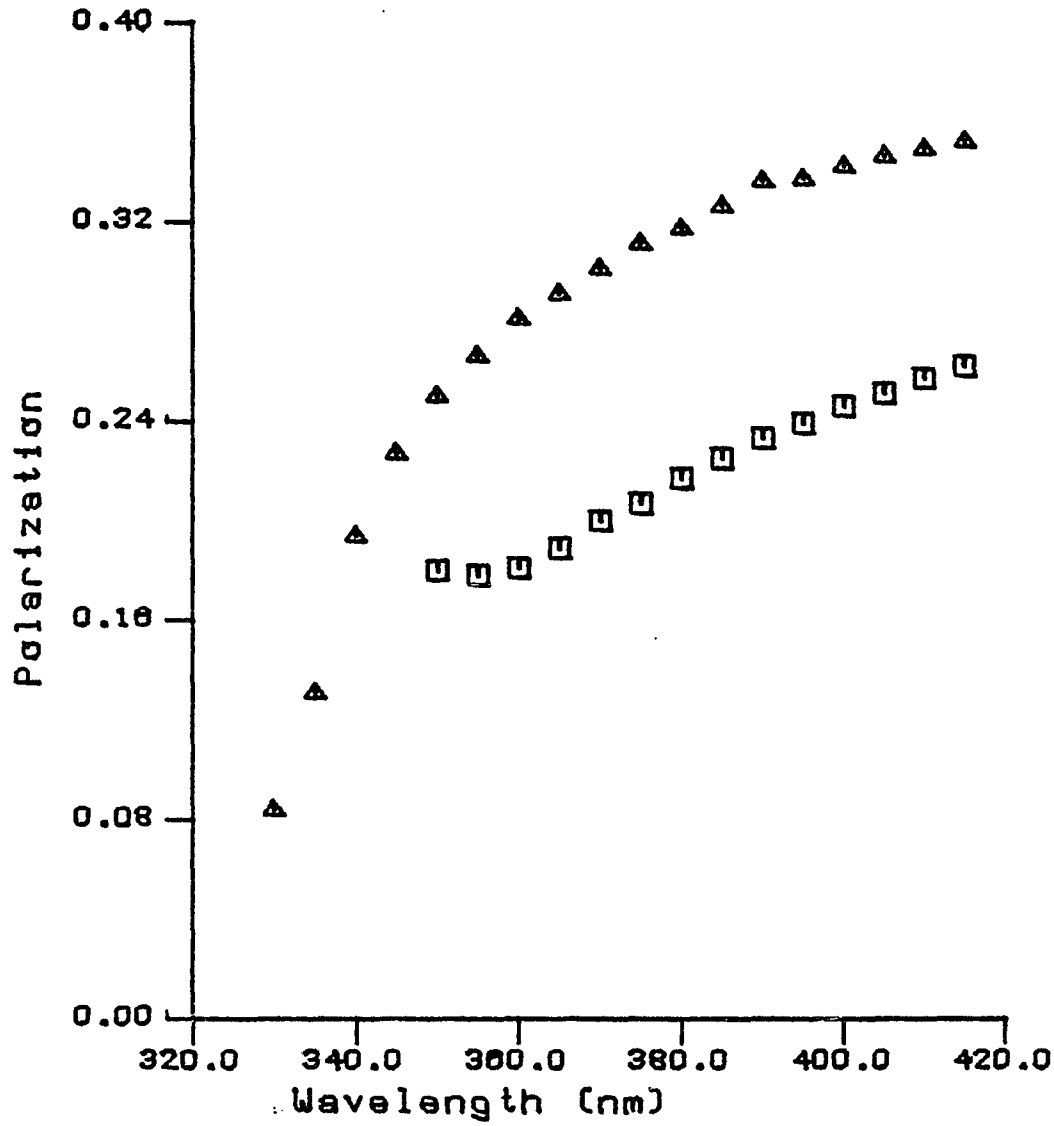

Figure 6. Polarization spectra, Zn-8-quinolinol complexes. Emission through long pass filter with 50%T at 518 nm Bandpass: 4nm. 1:1 complex (Δ); 2:1 complex (□)

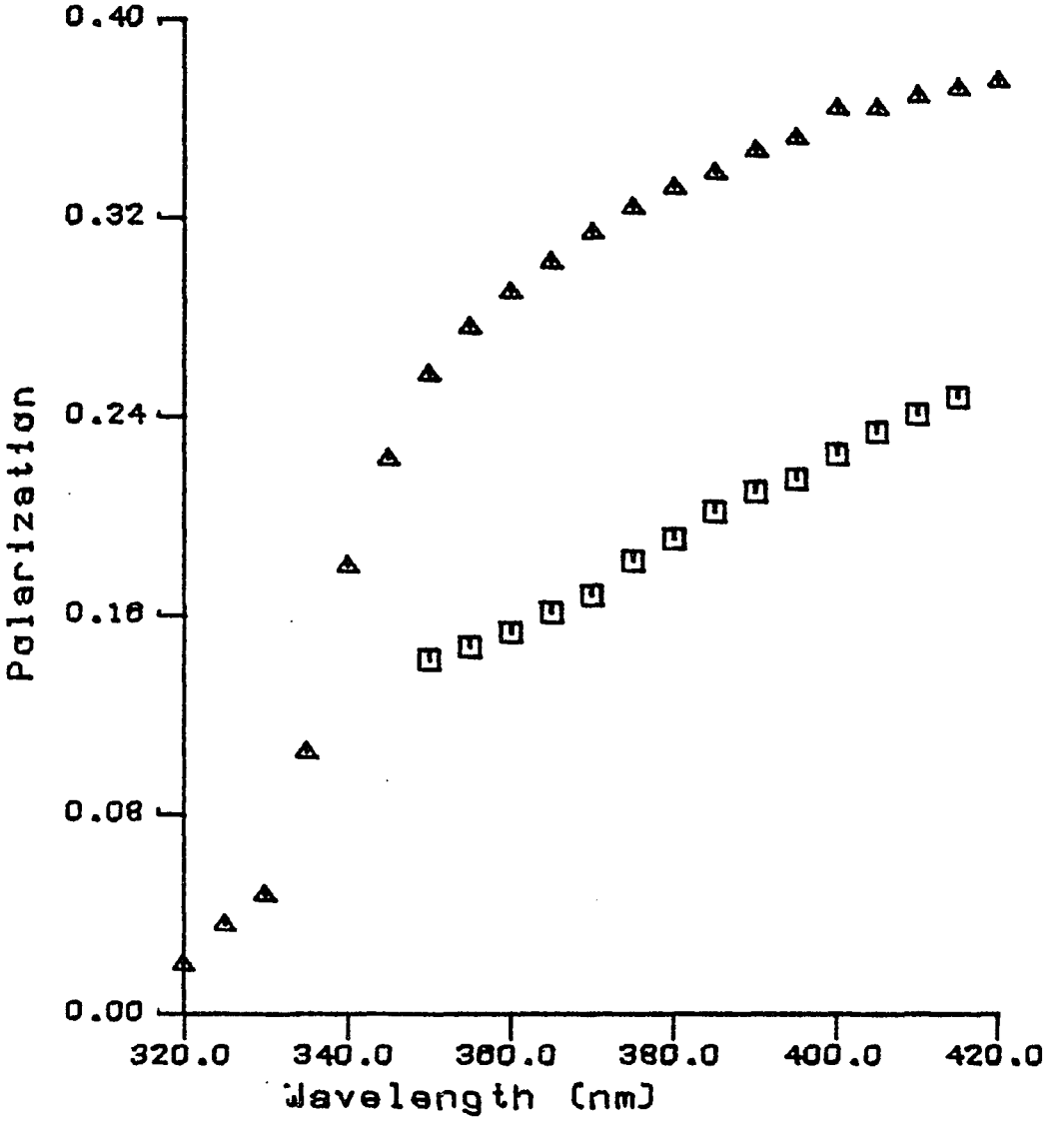

Figure 7. Polarization spectra, Mg-8-quinolinol complexes. Emission through long pass filter with 50%T at 518nm Bandpass: 4nm. 1:1 complex (▲); 2:1 complex (⊡)

wavelength is similar for all complexes although there are changes in the ratio of polarization for the 1:1 complex to the polarization of the limiting complex. Absorption and emission maxima shift slightly with the stoichiometry of the complexes. Maxima are summarized in Table 3.

Organic Bifluorophor

The polarization for p-cresol was 0.155; and the polarization for 4,4'methylene diphenol was 0.124. Excitation and emission wavelengths were 280 and 305 nm, respectively.

Discussion

Crown Ether

The fact that polarization is significantly lower for the dibenzo crown ether with two fluorophors than for the monobenzo crown with a single fluorophor is indicative of intramolecular energy transfer. The increase in polarization is consistent with a flatter structure for the K-DB18C6 complex relative to the free DB18C6 molecule. The angle between equivalent fluorophors is increased in the complexed form (Figure 1b). Using equations (2) and (3) the calculated angle z is 31.0°. However, since the square of cos 180° is the same as the square of cos 0° in equation (3), 31.0° may represent the deviation from 180° rather than from 0°. In view of the crystal structure for Na-DB18C6 $2H_2O$ (Bush), in which the dihedral angle between the planes of the benzene rings was reported to be 126.4°, it is reasonable to consider the deviation from planarity in this case. Therefore, the angle between emission transition moments, and thus between equivalent fluorophors in the complex is 149.0°.

Since there was no perturbation of the polarization spectrum upon complexation (Table 1b), the angle between the fluorophors was calculated assuming the transition moment is perpendicular to the plane of the fluorophor. The difference in polarization enabled us to distinguish the complexed from the free form of the crown ether without performing an extraction step. This difference could be useful analytically since it saves analysis time as well as enabling more accurate determinations of equilibrium constants. A major advantage is that the measurement process does not disturb the equilibrium distribution. This approach would be more widely applicable if solvents other than glycerol could be used. Unfortunately, rotational depolarization is rapid in less viscous solvents.

This data indicates that the potassium complexes are monomeric. There is no evidence of dimerization for either crown ether studied, although such structures have been proposed in alcohol solutions (Frensdorff; Mallinson). Dimers, with twice as many equivalent fluorophors in a complex, would exhibit decreased polarization due to increased probability of energy transfer.

Metal Complexes

The intrinsic polarization of 8-quinolinol and morin fluorescence was obtained from the 1:1 complexes. The decrease in polarization with increasing ligand-to-metal ratio indicates that excitation energy can transfer from one equivalent fluorophor to another providing the equivalent fluorophors are ligands bound to a common metal center. Energy transfer is predictable since the distance between equivalent ligands on the same metal center (Merritt) is much

less than the critical distance for Forster energy transfer. The critical radii for 8-quinolinates were calculated to be 11.4Å, 13.8Å, and 9.9Å for Al, Mg, and Zn complexes respectively using lifetime data obtained in dimethylformamide (Lytle).

As expected, the Mg and Zn complexes of 8-quinolinol have simiar limiting polarization values in the presence of excess ligand. Both of these metal ions form octahedral 2:1 quinolate complexes. The 3:1 Al complex has a lower limiting polarization since in this case the excitation energy can redistribute over all three equivalent fluorescent ligands. The difference in polarization for the 2:1 morin-Al complex is smaller than that for the 2:1 quinolates. In the morin system a limiting polarization was not observed, indicating that the 2:1 complex did not completely form in glycerol.

The extent to which fluorescence is depolarized by going from the 1:1 to the highest complex can be expressed in terms of the angle of extrinsic depolarization from equation (2). Calculated values for $\overline{\cos^2 w}$ for the quinolate complexes are included in Table 2. There should be a relationship between w and the structure of the complex. The expected values for $\overline{\cos^2 w}$ for solutions containing a single quinolate complex were calculated assuming the following:

a. The electronic properties of equivalent fluorescent ligands in a complex are not perturbed by the addition of successive ligands to the metal center.

b. The energy transfer process is fast relative to emission, which causes excitation energy to be randomly distributed among all the ligands. For instance, in a 3:1 complex, one-third of the excitation

Table 2

Variation in Experimental Values of $\overline{\cos^2 w}$ with Excitation Wavelength

a. Al

	Polarization		
	1:1	3:1	$\overline{\cos^2 w}$
λ (nm)			
360	0.310	0.095	0.524
370	0.327	0.111	0.544
380	0.342	0.125	0.559
390	0.350	0.137	0.575
400	0.359	0.152	0.595

b. Mg

	1:1	2:1	$\overline{\cos^2 w}$
λ (nm)			
370	0.301	0.200	0.760
380	0.317	0.217	0.773
390	0.336	0.233	0.778

c. Zn

	1:1	2:1	$\overline{\cos^2 w}$
λ (nm)			
370	0.314	0.168	0.672
380	0.332	0.191	0.700
390	0.347	0.210	0.717
400	0.364	0.225	0.725
410	0.369	0.241	0.749

energy would remain on the ligand originally excited while the other two ligands would each receive a third of the excitation energy. The general relationship was given in equation 3.

c. For octahedral complexes, the theoretical angle between ligands is 60°. If the emission transition moments are linear with respect to the 8-quinolinol structure, then z, the angle between transition moments of equivalent fluorophors (Equation 3) is also 60°. This angle assumes a trans 2:1 complex which is reasonable in a solvent such as glycerol which can itself act as a bidentate ligand. For tetrahedral complexes, the theoretical angle between ligands is 90°.

Since the limiting polarization is not reached for the morin complex, angle calculations were not attempted for that system. This simple model predicts $\overline{\cos^2 w} = 0.5$ for the 3:1 complex and 0.625 for the 2:1 octahedral complexes of 8-quinolinol. While trends are correct, the calculated values are smaller than the experimental values. The simple model used for the calculation is apparently not satisfactory. As the spectral shifts in Table 3 and wavelength dependence of $\overline{\cos^2 w}$ in Table 2 indicate, assumption (a) does not rigorously hold. The other assumptions, particularly (c), may also be oversimplifications.

Organic Bifluorophor

The methylene linkage does not perturb fluorescence for p-cresol and 4,4'methylenediphenol. In this case the molecule is probably free to rotate about the methylene linkage. In solution an average angle between transition moments could be determined, which could be of value for obtaining solution structural information.

Table 3

Wavelengths of Maximum Absorption and Emission for 8-quinolinol Complexes

		λ max (nm)	
Metal	Number of Ligands	Absorption	Emission
Al	1	367	475
Al	3	384	505
Zn	1	376	575
Zn	2	393	575
Mg	1	370	500
Mg	2	366	498

Conclusion

The systems studied demonstrate intramolecular energy transfer depolarization. This phenomenon can used to obtain both analytical and structural information. It is especially useful analytically in distinguishing components of a binary fluorophor without a separation step. It can also be used to distinguish between complexes differing in the number of fluorophors or in the angle between transition moments. Finally, it can distinguish monomeric from multimeric species which could be of value where speciation information is important.

REFERENCES

Argauer,R.J.; White,C.E. Spectrochim Acta, 1964, 20, 1323.

Bayer,E.; Albert,K.; Reiners,J.; Nieder,M.; Muller,D. J Chromatogr. 1983, 264, 197.

Bhatnagar,D.C.; Forster,L.S. Spectrochim Acta, 1965, 21, 1803.

Bidlingmeyer,B.A.; Deming,S.N.; Price,W.P.Jr.; Sachok,B.; Petrusek,M. J Chromatogr. 1979, 186, 419.

Bidlingmeyer,B.A. Liq Chromatogr. 1983, 1, 344.

Bij,C.; Horvath,C.; Melander,W.R.; Nahum,A. J Chromatogr. 1981, 203, 65.

Bush,M.A.; Truter,M.R. J Chem Soc.(B), 1971, 1440.

Bush,S.G.; Jorgenson, J.W.; Miller,M.L.; Linton,R.W. J Chromatogr. 1983, 260, 1.

Cantwell,F.F.; Puon,S. Anal Chem. 1979, 51, 623.

Carter,D.A.; Ohnesorge,W.E. Anal Chem. 1964, 36, 327.

Davis,L.E. Water Soluble Resins, 1968, Reinhold Press, N.Y.

DeArmond,M.K.; Carlin,C.M.; Huang,W.L. Inorg Chem. 1980, 19, 62.

Deming,S.N.; Kong,R.C. J Chromatogr. 1981, 217, 421.

Encyclopedia of Polymer Science and Technology, Vol. 10, 1968, Wiley Interscience, N.Y.

Forster,Th. Disc Faraday Soc. 1959, 27, 7.

Frensdorff,J. J Am Chem Soc. 1971, 93, 600.

Gilpin,R.K. Am Lab. 1982, 14(3), 104.

Gilpin,R.K.; Gangoda,M.E. J Chromatogr Sci. 1983, 21, 352.

Gilpin,R.K.; Squires,J.A. J Chromatogr Sci. 1981, 19, 195.

Gloor,R.; Johnson,E.L. J Chromatogr Sci. 1977, 15, 413.

Gordon,M; Ware,W.R.,Eds. The Exciplex, 1975, Academic Press, N.Y.

Hammers,W.E.; Verschoor,P.B.A. J Chromatogr. 1983, 282, 41.

Hearn,M.T.W. Adv in Chromatogr. 1980, 18, 59.

Hercules,D.M.,Ed. Fluorescence and Phosphorescence Analysis: Principles and Applications, 1966, Wiley Interscience, N.Y.

Herkstroeter,W.G.; Martic,P.A.; Hartman,S.E.; Williams,J.L.R.; Farid,S. J Polymer Sci, Polymer Chem Ed. 1983, 21, 2473.

Horvath,C.; Melander,W.; Molnar,I. J Chromatogr. 1976, 125, 129.

Ise,N.; Okubo,T.; Kunugi,S. Accts Chem Res. 1982, 15, 171.

Iskandarani,Z.; Pietrzyk,D.J. Anal Chem. 1982, 54, 1065.

Jandera,P.; Churacek,J.; Taraba,B. J Chromatogr. 1983, 262, 121.

Katyal,M. Tantala, 1968, 15, 95.

Katyal,M. Tantala, 1977, 24, 367.

Klotz,I.M. Adv in Chem Phys. 1978, 36, 109.

Knox,J.H.; Hartwick,R.A. J Chromatogr. 1981, 204, 3.

Kong,R.C.; Sachok,B.; Deming,S.N. J Chromatogr. 1980, 199, 307.

Kosower,E.M.; Kanety,H. J Am Chem Soc. 1978, 100, 4179.

Live,D.; Chan,S.I. J Am Chem Soc. 1971, 98, 3769.

Lochmuller,C.H.; Colborn,A.S.; Hunnicutt,M.L.; Harris,J.M. Anal Chem. 1983, 55, 1344.

Lytle,F.E.; Storey,D.R.; Juricich,M.E. Spectrochim Acta, 1973, 29A, 1357.

Mallinson, P.R.; Truter, M.R. J Chem Soc: Perkin II, 1972, 1818.

Melander,W.R.; Horvath,C. J Chromatogr. 1980, 201, 211.

Manning,G.S. Accts Chem Res. 1979, 12, 443.

Martic,P.A.; Daly,R.C.; Williams,J.L.R.; Farid,S. J Polymer Sci: Polymer Lett Ed. 1979, 17, 305.

Merritt,L.L.; Cady,R.T.; Mundy,B.W. Acta Cryst. 1954, 7, 473.

Ohnesorge,W.E.; Rogers,L.B. Spectrochim Acta, 1959, 15, 27.

Ohnesorge,W.E. J Inorg Nucl Chem. 1967, 29, 485.

Parker,C.A. Photoluminescence of Solutions, 1968, Elsevier, Amsterdam.

Pedersen,C.J. J Am Chem Soc. 1967, 89, 7017.

Popovych,O.; Rogers,L.B. Spectrochim Acta, 1960, 16, 49.

Pranis,R.A.; Klotz,I.M. Biopolymers, 1977, 16, 299.

Prieto,N.E.; Martin,C.R. J Electrochem Soc. in press.

Ramanathan,G.V. J Chem Phys. 1983, 78, 3223.

Rosen,M.J. Surfactants and Interfacial Phenomena, 1978, John Wiley & Sons, N.Y.

Scott,R.P.W.; Simpson,C.R. J Chromatogr. 1980, 197, 11.

Seitz,W.R. CRC Rev Anal Chem. 1980, 8, 367.

Shizuka,H.; Takada,K.; Morita,T. J Phys Chem. 1980, 84, 994.

Sisido,M.; Akiyama,K.; Imanishi,Y.; Klotz,I.M. Macromolecules, 1984, 17, 198.

Smith,R.M.; Martell,A.E. Critical Stability Constants, 1975, Plenum Press, N.Y.

Stepanova,A.G.; Tropina,P.L.; Fakeeva,O.A. Russ J Anal Chem. 1978, 33, 1782.

Stevens,H.M. Anal Chim Acta, 1959, 20, 389.

Stranahan,J.J.; Deming,S.N. Anal Chem. 1982, 54, 2251.

Stryer,L. Ann Rev Biochem. 1978, 47, 819.

Taha,I.A.; Morawetz,H.J. J Am Chem Soc. 1971, 93, 829.

Tang,M.; Deming,S.N. Anal Chem. 1983, 55, 425.

Tchapla,A.; Colin,H.; Guiochon,G. Anal Chem. 1984, 56, 621.

Thomas,J.K. Chem Rev. 1980, 80, 283.

Turro,N.J.; Okubo,T. J Am Chem Soc. 1982, 104, 2985.

Turro,N.J.; Okubo,T. J Phys Chem. 1982, 86, 1535.

Turro,N.J.; Pierola,I.F. J Phys Chem. 1983, 87, 2420.

Vink,H. J Chem Soc: Faraday Trans I, 1983, 79, 1403.

Ware,W.R., Chakrabarti,S.K. J Chem Phys. 1971, 55, 5494.

Wise,S.A.; May,W.E. Anal Chem. 1983, 55, 1479.

Wong,E., personal communication.

Zero,K.; Cyr,D.; Ware,B.R. J Chem Phys. 1983, 79, 3602.